



Dual transcriptomic analysis reveals metabolic changes associated with differential persistence of human pathogenic bacteria in leaves of *Arabidopsis* and lettuce

Cristián Jacob ^{1,2,3,*}, André C. Velásquez,⁴ Nikhil A. Josh,⁵ Matthew Settles,⁵ Sheng Yang He,^{4,6} and Maeli Melotto ¹

¹Department of Plant Sciences, University of California, Davis, Davis, CA 95616, USA

²Department of Plant Sciences, Horticulture and Agronomy Graduate Group, University of California, Davis, Davis, CA 95616, USA

³Departamento de Ciencias Vegetales, Facultad de Agronomía e Ingeniería Forestal, Pontificia Universidad Católica de Chile, Santiago 7820436, Chile

⁴Department of Biology, Howard Hughes Medical Institute, Duke University, Durham, NC 27708, USA

⁵Bioinformatics Core Facility in the Genome Center, University of California, Davis, Davis, CA 95616, USA and

⁶Department of Biology, Duke University, Durham, NC 27708, USA

*Corresponding author: Pontificia Universidad Católica de Chile, Santiago, Chile. Email: cjjacob@uc.cl

Abstract

Understanding the molecular determinants underlying the interaction between the leaf and human pathogenic bacteria is key to provide the foundation to develop science-based strategies to prevent or decrease the pathogen contamination of leafy greens. In this study, we conducted a dual RNA-sequencing analysis to simultaneously define changes in the transcriptomic profiles of the plant and the bacterium when they come in contact. We used an economically relevant vegetable crop, lettuce (*Lactuca sativa* L. cultivar Salinas), and a model plant, *Arabidopsis thaliana* Col-0, as well as two pathogenic bacterial strains that cause disease outbreaks associated with fresh produce, *Escherichia coli* O157:H7 and *Salmonella enterica* serovar Typhimurium 14028s (STm 14028s). We observed commonalities and specificities in the modulation of biological processes between *Arabidopsis* and lettuce and between O157:H7 and STm 14028s during early stages of the interaction. We detected a larger alteration of gene expression at the whole transcriptome level in lettuce and *Arabidopsis* at 24 h post inoculation with STm 14028s compared to that with O157:H7. In addition, bacterial transcriptomic adjustments were substantially larger in *Arabidopsis* than in lettuce. Bacterial transcriptome was affected at a larger extent in the first 4 h compared to the subsequent 20 h after inoculation. Overall, we gained valuable knowledge about the responses and counter-responses of both bacterial pathogen and plant host when these bacteria are residing in the leaf intercellular space. These findings and the public genomic resources generated in this study are valuable for additional data mining.

Keywords: dual transcriptomic profiling; *Salmonella enterica*; *Escherichia coli* O157:H7; disease outbreak; food safety

Introduction

Globally, according to the World Health Organization (WHO), the most frequent causes of foodborne illness are diarrheal disease agents, primarily non-typhoidal *Salmonella enterica* and enteropathogenic *Escherichia coli*, which in 2010 caused an estimated 230,000 deaths (WHO 2015). Outbreaks of *S. enterica* and pathogenic *E. coli* associated with the intake of uncooked produce are reported every year in Europe (Callejón et al. 2015) and in the United States (Bennett et al. 2018). For example, from 1998 to 2013, there were 972 raw produce-linked outbreaks reported to the Foodborne Disease Outbreak Surveillance System managed by the Center for Disease Control and Prevention, which accounted for 34,674 illnesses, 2,315 hospitalizations, and 72 deaths in the United States (Bennett et al. 2018). In particular, leafy greens products from California, mainly lettuce and spinach, were involved in 46 outbreaks from 1996 to 2016, where the most frequent microbiological hazards were *E. coli* and *Salmonella* (Turner et al. 2019).

Over the last two decades, an extraordinary effort has been made to gain an understanding of the biological processes underlying the contamination of fresh produce by *S. enterica* and *E. coli* (Hernández-Reyes and Schikora 2013; Sapers and Doyle 2014). Specifically, biochemical, molecular, and genetic studies have revealed a significant contribution of the plant innate immune response against human pathogenic bacteria in the phyllosphere (Schikora et al. 2011; Melotto et al. 2014; Jo and Park 2019). After exposure to *Salmonella* or *E. coli* serotype O157:H7 (hereafter O157:H7), pattern-triggered immunity responses (i.e., reactive oxygen species burst, stomatal closure, activation of mitogen-activated protein kinases, ethylene, salicylic acid, and jasmonic acid signaling, expression of pathogenicity-related proteins, and callose deposition) have been observed in *Arabidopsis* (Thilmony et al. 2006; Schikora et al. 2008; Garcia et al. 2014), tobacco (Shirron and Yaron 2011), lettuce (Roy et al. 2013; Jacob and Melotto 2019; Jechalke et al. 2019), and *Medicago truncatula* (Jayaraman et al. 2014). Research has also elucidated numerous molecular

Received: March 03, 2021. Accepted: September 09, 2021

© The Author(s) 2021. Published by Oxford University Press on behalf of Genetics Society of America.

This is an Open Access article distributed under the terms of the Creative Commons Attribution License (<https://creativecommons.org/licenses/by/4.0/>), which permits unrestricted reuse, distribution, and reproduction in any medium, provided the original work is properly cited.

determinants involved in the colonization of bacteria in/on leaves (Holden *et al.* 2009; Brandl *et al.* 2013; Yaron and Römling 2014). For instance, components of the bacterial extracellular matrix, such as curli, cellulose, and colanic acid (CA) have a significant role in the attachment and/or persistence of O157:H7 in lettuce (Fink *et al.* 2012) and spinach (Saldaña *et al.* 2011; Macarasin *et al.* 2013) and of *S. enterica* serovars Enteritidis and Newport in alfalfa sprouts (Barak *et al.* 2007). In addition, significant modulation of the expression of genes related to antimicrobial resistance, oxidative stress, motility, and carbon, nitrogen, and sulfur transport and metabolism has been observed in O157:H7 and *S. enterica* serovar Weltevreden after inoculation on lettuce leaves (Fink *et al.* 2012; van der Linden *et al.* 2016) and alfalfa sprouts (Brankatschk *et al.* 2014), respectively. Furthermore, the contribution of structural type 3 secretion system (T3SS) and type 3 effector (T3E) proteins in *Salmonella* adhesion, internalization, and persistence in/on the phyllosphere has been widely investigated (Schikora *et al.* 2011; Shirron and Yaron 2011; Chalupowicz *et al.* 2018; Montano *et al.* 2020). Nevertheless, the specific roles of certain T3SS and T3E proteins remain controversial and might be pathosystem specific.

Microarray- and RNA-seq-based transcriptomic studies have contributed substantially to unravelling the molecular processes occurring during the interaction between the plant and *S. enterica* or *E. coli* (Thilmony *et al.* 2006; Schikora *et al.* 2011; Fink *et al.* 2012; Brankatschk *et al.* 2014; Garcia *et al.* 2014; Jayaraman *et al.* 2014; Landstorfer *et al.* 2014; Van der Linden *et al.* 2016; Jechalke *et al.* 2019). Nonetheless, these studies have limited their genome-wide gene expression analyses to only one of the organisms involved in the interaction, the host or the pathogen, over time. With current high-throughput RNA-seq tools and bioinformatics resources, dual transcriptomic studies can be conducted, in which deep transcriptomic profiles of the microbial and the eukaryotic host cells are simultaneously captured (Saliba *et al.* 2017; Westermann *et al.* 2017). Bioinformatics pipelines have been developed and described in detail to analyze dual RNA-seq experiments where total reads are preprocessed, mapped to each or in parallel to both reference genomes, counted, and finally normalized for downstream analysis (Marsh *et al.* 2018; Nobori *et al.* 2018). Dual RNA-seq technical approaches have been applied in a variety of host/pathogen combinations, such as *Mus musculus*/*Streptococcus pneumoniae* (Ritchie and Evans 2019), *Salmo salar*/*Piscirickettsia salmonis* (Valenzuela-Miranda and Gallardo-Escárate 2018), *Eucalyptus nitens*/*Phytophthora cinnamomi* (Meyer *et al.* 2016), and *M. truncatula*/*Erysiphe pisi* (Gupta *et al.* 2020).

In our study, we aimed to simultaneously obtain the transcriptomic profiles of the two human pathogenic bacteria most frequently linked to disease outbreaks, *Salmonella* and *E. coli*, with the model plant *Arabidopsis* and the vegetable crop lettuce, which has been the vehicle for disease outbreaks. These multiple datasets enabled us to explore shared and unique metabolic processes that are modulated at different times in several bacterium-plant combinations. In addition, we identified multiple bacterial and plant genes with potential key roles in the leaf colonization by these two human pathogenic bacteria.

Materials and methods

Plant material and growth conditions

Arabidopsis (*Arabidopsis thaliana* [L.] Heynh. ecotype Col-0) and lettuce (*Lactuca sativa* L. cultivar Salinas) were grown as previously described (Jacob *et al.* 2017; Jacob and Melotto 2019). The iceberg lettuce cultivar Salinas was chosen for this study because

it is extensively used in genetics studies and breeding efforts; its genome is also sequenced and annotated as a reference for this species (Reyes-Chin-Wo *et al.* 2017). *Arabidopsis* seeds were incubated for 2 days at 4°C for stratification. Lettuce seeds were germinated directly on water-soaked paper in square Petri dishes and maintained at 20°C for 2 days. Subsequently, *Arabidopsis* seeds were sown in 7.62 cm² pots (3"; Kord Products, Toronto, Canada) containing a soil mix (Sun Gro[®] Sunshine[®] #1 Grower Mix with RESILIENCE[™], Agawam, MA, USA) and germinated lettuce seeds were transferred to the same pot type filled with the same soil mix. The soil used for *Arabidopsis* was previously soaked overnight with a fungus gnat prevention solution, 1g/l Gnatrol WDG (Valent, Canada), and to avoid the contact of the leaves with the soil, a layer of fine vermiculite was added on the surface, which was then covered with a fiberglass mesh screen. *Arabidopsis* growth chamber conditions were 22 ± 1°C, 65 ± 5% relative humidity (RH), and photosynthetically active light intensity of 90 ± 10 μmol/m²/s. Lettuce plants were grown at 19 ± 1°C, 75 ± 4% RH, and photosynthetically active light intensity of 240 ± 10 μmol/m²/s. Both species were grown with a 12-h photoperiod. One liter of tap water was added to the tray two to three times per week depending on the developmental stage of the plants. At 10 days post germination, lettuce plants were fertilized with 0.05 g/plant of fertilizer (Multi-Purpose 19-11-21; Peters[®]Excel, OH, USA) dissolved in the irrigation water.

Bacterial strains and inoculation procedure

The non-typhoid *S. enterica* subspecies *enterica* serovar Typhimurium strain 14028s (Porwollik *et al.* 2014) and the enterohemorrhagic *E. coli* serotype O157:H7 strain 86-24 (Sperandio *et al.* 2001) were grown in Low Salt Luria-Bertani medium (10 g/l tryptone, 5 g/l yeast extract, 5 g/l NaCl, pH 7.0) at 28°C. Medium supplemented with 50 μg/ml of streptomycin was used to grow O157:H7. To minimize bacterial stress due to centrifugation, the inoculum was prepared by directly transferring the bacterial cultures from the solid medium into a sterile 1 mM MgCl₂ aqueous solution. The inoculum was infiltrated into the intercellular space of the leaf using a needleless syringe, as previously described by Katagiri *et al.* (2002). Inoculations were conducted in 3.5-week-old *Arabidopsis* plants and 4-week-old lettuce plants (Supplementary Figure S1, A and B). To determine the effect of inoculum concentration on bacterial persistence and optimum recovery of bacterium transcripts for downstream analyses, *Arabidopsis* plants were inoculated with four levels of bacterial inoculum, 1 × 10⁶, 10⁷, 10⁸, or 10⁹ CFU/ml. For RNA extraction, *Arabidopsis* plants were inoculated with a low (5 × 10⁶ CFU/ml) and a high (1 × 10⁹ CFU/ml) inoculum concentration, while lettuce plants were inoculated with a high inoculum concentration only. Mock inoculation with 1 mM MgCl₂ was used as the negative control. Each plant was used to determine bacterial population size and extract RNA for transcriptomic profiling. The analysis workflow is depicted in Supplementary Figure S1C.

Bacterial enumeration

Leaves from the same plants used for RNA extraction were collected to determine the size of the apoplastic bacterial population following the serial dilution method as previously described (Jacob *et al.* 2017).

RNA extraction and quality assessment

Total RNA was extracted from fresh inoculum immediately before the inoculations. Three 1 ml samples (n = 3) were centrifuged at 3000 × g for 2 min at 20°C to recover bacterial cell pellets that

were immediately used for RNA extraction using the RiboPure™-Bacteria Kit (Ambion, Austin TX, USA) according to the manufacturer's instructions.

RNA from inoculated leaves was extracted at 4 and 24 h post inoculation (HPI). Whole leaves (*Arabidopsis*) or leaf pieces (lettuce) were excised from three separate plants for each sampling point for each treatment ($n=3$). Immediately after collection, leaf material was placed into 2 ml self-standing, impact-resistant tubes (USA Scientific Inc., Ocala, FL, USA) containing three Zirconium beads (3 mm diameter; Glen Mills Inc., Clifton, NJ, USA), frozen in liquid nitrogen, and stored at -80°C . Leaf tissue was mechanically disrupted twice using a tissue grinder (Mixer Mill MM 400; Retsch, Haan, Germany) for 1 min at 30 Hz; the tissue was kept frozen throughout the procedure. Tubes were transferred to ice after tissue disruption and 1 ml of TRIzol reagent (Thermo Fisher Scientific, Waltham, MA, USA) was added. After incubation for 5 min, 200 μl of chloroform was added, the sample was vortexed for 20 seconds, and then centrifuged for 15 min at $16,000 \times g$ and 4°C . The clear phase, normally approximately 500 μl , was transferred to a new tube and an equal volume of refrigerated RNase-free 100% (v/v) ethanol was added. The solution was then loaded into a clean-up column of the Direct-Zol™ RNA Miniprep kit (Zymo Research, Irvine, CA, USA) for RNA purification according to the manufacturer's protocols.

All samples were subjected to a DNase treatment with the Turbo DNA-free kit (Ambion, Austin, TX, USA) and total RNA was quantified using a Qubit 3.0 fluorometer (Life Technologies, Carlsbad, CA, USA) and NanoDrop 2000c spectrophotometer (Thermo Scientific, Waltham, MA, USA). RNA quality was also assessed using a 2100 Bioanalyzer (Agilent, Santa Clara, CA, USA) and 1% agarose electrophoresis containing 1% (v/v) bleach (Clorox, Oakland, CA, USA) as recommended by Aranda et al. (2012).

Library preparation and sequencing

Libraries from *Arabidopsis* samples were prepared using the Ovation Universal RNA-Seq System (NuGEN, San Carlos, CA, USA), with additional custom AnyDeplete (NuGEN, San Carlos, CA, USA) probes (Nobori et al. 2018). RNA extracted from leaves inoculated with 1×10^9 CFU/ml were subjected to bacterial rRNA depletion with the Ribo-Zero™ rRNA Removal Kit, Bacteria (Illumina, San Diego, CA, USA). Libraries from lettuce samples were prepared using both Bacteria and Plant Ribo-Zero™ rRNA Removal Kits (Illumina, San Diego, CA, USA). Libraries from bacterial inoculum were prepared using the Ribo-Zero™ rRNA Removal Kits, Bacteria (Illumina, San Diego, CA, USA).

Sequencing libraries were quality controlled and quantified using a combination of Qubit dsDNA HS (Thermo Fisher Scientific, Waltham, MA, USA) and Advanced Analytical Fragment Analyzer High Sensitivity NGS DNA (Agilent, Santa Clara, CA, USA) assays. Sequencing was conducted in an Illumina HiSeq 4000 flow cell with a 1×50 -bp single read format using HiSeq 4000 SBS reagents. Base calling was done by Illumina Real Time Analysis (RTA) v2.7.7 and the RTA output was demultiplexed and converted to FastQ format with the Illumina Bcl2fastq v2.19.1 software.

Reads processing

Preprocessing of reads, including filtering of rRNA, adapter trimming, and quality-based trimming (a Phred score of 20 was used as the threshold for the average score in a sliding window, with a minimum length of 20 bp) was conducted using the HTStream (<https://github.com/s4hts/HTStream>; accessed October, 2021)

software. Subsequently, reads were simultaneously mapped to the sequenced genomes of three species, one plant species [*Arabidopsis* (TAIR10) or lettuce (LsV8)] and the two bacterial species [O157:H7 (GCA_000978845.1) and STm 14028s (GCA_000783815.1)] using the default parameter of the STAR RNA-Seq aligner version 2.5.2b. This approach was conducted to allow for the best alignment call for each read. Owing to the high redundancy of the bacterial genomes, the same read can map to both genomes if mapping were not done simultaneously, increasing the number of false positive alignments. Simultaneous mapping to all three genomes allows the aligner software to find the best match in only one genome providing the best alignment possible for this large dataset. The number of reads mapped to each genome is listed in Supplementary Table S1. Finally, the number of reads assigned to each gene was determined and read counts were normalized with the Log₂ counts per million (CPM) normalization method (Law et al. 2018).

Data analysis

To assess the interaction between the factors “inoculum concentration” and “days post inoculation” on the bacterial population, the data were subjected to a two-way analysis of variance (ANOVA) for each combination of plant and bacterium. Due to the significant interaction between these two factors ($P < 0.0001$) in all plant-bacterium combinations, we proceeded with assessing statistically significant changes in the bacterial population at the sampling points for each inoculum concentration within plant-bacterium combinations using ANOVA, followed by comparisons of multiple means using Tukey's test with a significance threshold of $\alpha = 0.05$.

The variation among replicates was evaluated with the correlation analyses multidimensional scaling (MDS) plot (Supplementary Figure S2) and Spearman's correlation test (Supplementary Figure S3) using the normalized read counts of each sample. All MDS plots (Supplementary Figure S2) show data from all treatments due to the simultaneous mapping of reads to both plant and bacterial genomes described above. Plots were generated with the R packages edgeR version 3.18.1 (MDS) and heatmap.2 (Spearman's correlation). Genes with expression values of 1 CPM or greater in at least five samples were kept for downstream analysis.

Differential expression was tested using a single factor ANOVA model in the limma package v3.32.10 of R v3.4.4. (Law et al. 2018). Significantly differentially expressed genes (DEGs) were considered when genes had a Benjamini-Hochberg false discovery rate (Benjamini and Hochberg 1995) with an adjusted P-value of < 0.001 for plant genes and < 0.05 for bacterial genes and with a Log₂ fold change (FC) > 1 or < -1 . Unique and shared significantly up or downregulated genes between treatments were obtained using the software InteractiVenn (<http://www.interactivenet.net/>; accessed October, 2021; Heberle et al. 2015) and plots showing the number of intersecting DEGs were constructed based on the UpSet plots from Lex et al. (2014).

Gene ontology (GO) enrichment analysis of significant DEGs of *Arabidopsis* and lettuce was conducted using the GO Consortium tool PANTHER14.1 Classification System (Mi et al., 2021) and Blast2GO software (Götz et al. 2008), respectively. Additionally, we used the corresponding *Arabidopsis* orthologous genes of the lettuce genes reported by Reyes-Chin-Wo et al. (2017). Predicted lettuce proteins were BLASTed against *A. thaliana* TAIR10 proteins with BLASTp (threshold E-value = 1×10^{-10}) to find homologous sequences. Out of the total number of predicted lettuce genes,

29,681 (76.27%) genes showed similarity to Arabidopsis TAIR10 annotations (Reyes-Chin-Wo *et al.* 2017).

Metabolic pathway reconstruction and hierarchical clustering analyses of plant DEGs were performed with the MapMan 3.5.1R2 (Thimm *et al.* 2004) and heatmap.2 R package, respectively, using default settings. To analyze the relationship between treatments, comprehensive lists of 7112 Arabidopsis genes and 7469 lettuce genes containing all DEGs throughout the samples were used in the hierarchical cluster analysis. Using the Arabidopsis orthologs of lettuce genes we were able to compare all the treatments according to genes involved in biological processes related to primary and secondary metabolism and biotic stress, which were selected based on MapMan 3.5.1R2 classification and genes comprising enriched GO terms.

To analyze the relationship between bacterial transcriptomic changes among the treatments, we conducted hierarchical clustering analyses using lists comprising all DEGs throughout the O157:H7 samples (2420 DEGs) and the STm 14028s samples (2887 DEGs) using the R package heatmap.2. Metabolic reconstruction of bacterial responses to different nutritional environments were made using the KEGG Mapper tool (Kanehisa and Sato 2020; <https://www.kegg.jp/kegg/mapper/reconstruct.html>; accessed October, 2021). First, KEGG protein IDs were obtained using the protein sequences available in each bacterial genome annotation resources as an input for the KofamKOALA tool with the threshold $E\text{-value} = 1 \times e^{-5}$ (Aramaki *et al.* 2020; <https://www.genome.jp/tools/kofamkoala/>; accessed October, 2021). Second, the KEGG IDs were linked to the corresponding DEG. KEGG IDs were used as input for reconstructing pathways using KEGG Mapper. Finally, we used the mapping results to run a KEGG pathway enrichment analysis using the hypergeometric test for over-representation of success as previously described (Chen *et al.* 2015).

Results and discussion

Optimum inoculation dosage for dual transcriptomic analysis

To perform a dual transcriptomic analysis, it is crucial to estimate the relative concentration of both bacterial and host RNA in the sample. This estimate can inform the required sequencing depth and adjustments in the inoculation level to obtain enough bacterial read counts for downstream analyses (Westermann *et al.* 2017). Thus, we inoculated Arabidopsis and lettuce with a range of inoculum concentrations from 1×10^6 to 10^9 CFU/ml and assessed bacterial population kinetics over 14 days post-inoculation (DPI). Although the initial bacterial population sizes at the day of inoculation (0 DPI) of both O157:H7 and STm 14028s were different, at 14 DPI their population sizes reached comparable values independently of the inoculum concentration (Figure 1).

Previously, we observed that a bacterial population size of at least 1×10^6 CFU/cm² leaf is required to yield a sufficient number of bacterial reads for downstream bioinformatics analysis (Nobori *et al.* 2018). This level was only reached in leaves inoculated with 1×10^9 CFU/ml at 0 and 1 DPI in both Arabidopsis and lettuce (Figure 1), resulting in a range of 5.1–11.9 and 1.9–4.6 million bacterial reads in leaf samples of Arabidopsis and lettuce, respectively (Supplementary Table S1), which is enough to detect significantly DEGs (Haas *et al.* 2012). Notably, inoculated leaves showed no macroscopic symptoms during the sampling period (Supplementary Figure S4). The use of a high inoculum concentration is not entirely unrealistic as focal contamination of leaves with fecal matter of super-shedder animals (*e.g.*, swine, cattle) or

wild birds (*e.g.*, pheasants, gull, goose) can carry high levels of bacteria ($1 \times 10^{7-9}$ CFU/g feces; Brichta-Harhay *et al.* 2007; Gopinath *et al.* 2012; Smith *et al.* 2020), which may spread to adjacent plants in the field. Nonetheless, we also performed a transcriptomic analysis of Arabidopsis leaves inoculated with a substantially lower bacterial concentration (5×10^6 CFU/ml) to assess the effect of inoculum concentrations in the plant transcriptomic profile.

Transcriptomic changes in Arabidopsis after inoculation with low bacterial concentration

The bacterial populations after infiltration with low concentration inoculum (5×10^6 CFU/ml; Figure 1A) were insufficient to capture the number of bacterial reads for DEG analysis (Supplementary Table S1). Nevertheless, using this condition, we observed significant changes in the transcription of Arabidopsis genes at the whole-genome scale (Figure 2; Dataset S03). When comparing each bacterial treatment with the mock control at each time point, we observed that O157:H7 modulated a higher number (2343) of genes at 4 HPI and STm 14028s modulated a higher number of genes (3089) at 24 HPI (Table 1; see Dataset S01).

Broadly, the GO enrichment analysis revealed that these bacteria induce changes in Arabidopsis metabolism and stress responses when compared to the mock control (Dataset S02). These results prompted us to re-construct the metabolic maps for these processes and to compare the treatments through heatmaps and hierarchical analysis based on DEGs associated with metabolism and stress responses. These analyses showed that O157:H7 stimulated changes in a large amount of DEGs involved in primary metabolism (Figure 3 and Supplementary Figure S5; Dataset S04) and plant responses to biotic stress (Figure 4 and Supplementary Figure S6; Dataset S05) at 4 HPI, while STm 14028s modulated a higher number of genes in these categories at 24 HPI (Figures 3 and 4).

Plants inoculated with STm 14028s or O157:H7 exhibited an overall reduction of photosynthesis reactions, which was accompanied by a downregulation in the expression of genes associated with other primary metabolic pathways (Figure 3 and Supplementary Figure S5). Furthermore, Arabidopsis interaction with STm 14028s and O157:H7 significantly induced the expression of genes involved in aging and leaf senescence, suggesting a disruption of normal leaf growth and development. Plants inoculated with O157:H7 exhibited an induction of the genes PYRUVATE, ORTHOPHOSPHATE DIKINASE (PPDK), which is involved in nitrogen remobilization during leaf senescence (Taylor *et al.* 2010), and SENESCENCE-ASSOCIATED PROTEIN (AAF). The inoculation of leaves with STm 14028s caused the upregulation of the SENESCENCE-ASSOCIATED GENES (SAG) 13, 20, 21, and 101.

It is widely theorized that during plant–pathogen interactions, growth–defense tradeoffs exist due to limited resources and that the balance between these two factors is regulated by phytohormone crosstalk (Huot *et al.* 2014). Accordingly, our analyses show that, at 24 HPI, most of the DEGs associated with plant defense signaling pathways are upregulated (Figure 4 and Supplementary Figure S6), which is also illustrated by the enriched GO terms associated with plant defenses among upregulated genes (Dataset S02).

Overlap analysis of DEG datasets

Next, we sought to determine the extent of the overlap between the DEGs identified by two-way comparisons (*i.e.*, bacterium versus mock). This analysis revealed common and unique

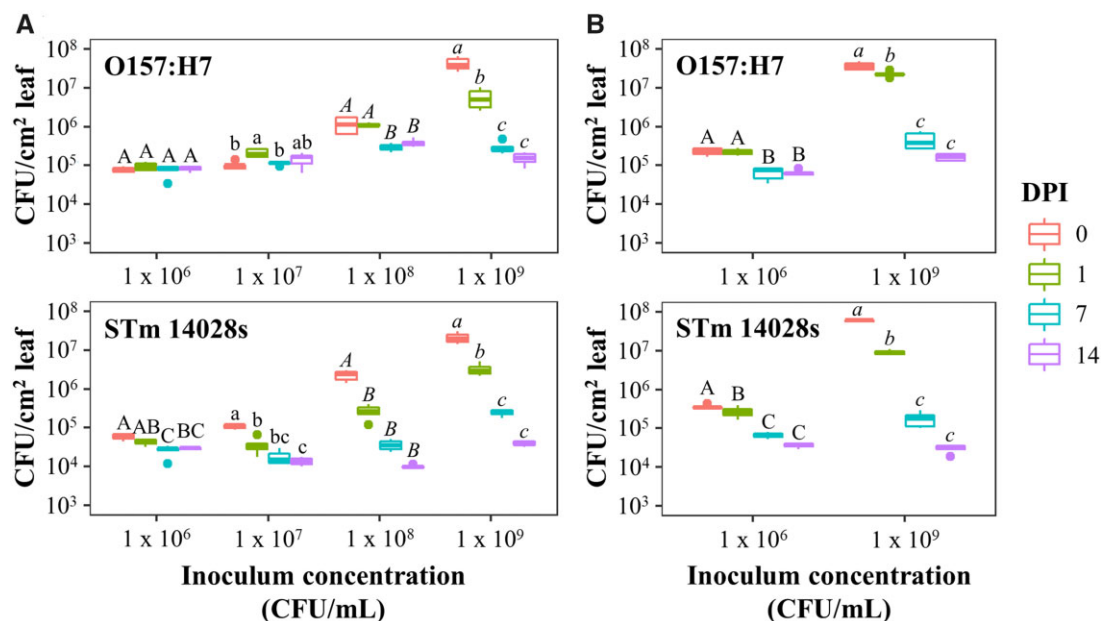


Figure 1 *Escherichia coli* O157:H7 and *Salmonella enterica* Typhimurium 14028s persistence in Arabidopsis (A) and lettuce (B) leaves after infiltration with different concentrations of inoculum (1×10^6 , 10^7 , 10^8 , or 10^9 CFU/ml). Leaves were surface sterilized, except at 0 days post inoculation (DPI), and serial dilution plating was conducted to quantify the bacterial population in the intercellular space. Three plants were used for each sample point ($n = 3$). Different letters on the top of adjacent data points (i.e., within the inoculum concentration groups) indicate significant statistical differences among the means, as calculated with ANOVA followed by Tukey's test ($\alpha = 0.05$).

modulation of the Arabidopsis transcriptome by bacterial species (Supplementary Figure S7; Dataset S06).

Genes involved in Arabidopsis response to both STm 14028s and O157:H7

To identify Arabidopsis genes that were modulated by both bacteria, we conducted an intersect analysis summarized in Supplementary Figure S7A. At 4 HPI, 102 and 477 Arabidopsis genes were up- and downregulated respectively, whereas at 24 HPI, 243 and 304 were up- and downregulated, respectively (Dataset S06). Arabidopsis genes commonly upregulated by both STm 14028s and O157:H7 were associated with GO terms involving response against biotic and abiotic stressors as early as 4 HPI, which continued to be enriched until 24 HPI. At this later time point, additional GO terms associated with plant immune response and signaling (such as protein phosphorylation and folding) were enriched (Dataset S07). The genes commonly repressed by these pathogens belong to enriched GO terms related to gene expression, mRNA processing, and primary metabolism at 4 HPI, whereas photosynthesis, carbohydrate metabolism, and cold acclimation associated GO terms were enriched at 24 HPI (Dataset S07).

Common transcriptional modulation in plants exposed to various bacteria has been previously reported. For instance, approximately 30% of *M. truncatula* DEGs are commonly regulated in response to cocktails of O157:H7 strains and *S. enterica* serovars, with a large proportion of genes related to pathogen defense being regulated similarly by these bacteria (Jayaraman et al. 2014). Likewise, Schikora et al. (2011) detected 164 overlapping DEGs in 14-day-old Arabidopsis Col-0 seedlings at 2 HPI with STm 14028s, the non-pathogenic *E. coli* strain DH5 α , and the phytopathogen *Pseudomonas syringae* pv. *tomato* DC3000. Our dataset has some overlap with the data reported by Schikora et al. (2011), in which 11.6 and 4.3% of the 164 DEGs observed by Schikora and collaborators were also differentially expressed in our plants at 4 HPI

with O157:H7 and STm 14028s, respectively, while at 24 HPI, these values increased to 12.8 and 43.9% (Dataset S08). Altogether, these findings confirm the existence of a basal response to bacterial-caused stress in Arabidopsis Col-0 ecotype. However, certain biological processes were uniquely altered by either O157:H7 or STm 14028s as described below.

Genes involved in Arabidopsis response unique to either STm 14028s or O157:H7

In general, O157:H7 modulated more genes than STm 14028s at 4 HPI and the opposite was observed at 24 HPI (Table 1). Likewise, the number of genes uniquely modulated by O157:H7 was considerably larger than that modulated by STm 14028s at 4 HPI, whereas this trend was reversed at 24 HPI when the number of genes uniquely by STm 14028s was considerably larger (Dataset S06).

O157:H7 modulated process. The greatest metabolic changes in response to O157:H7 occurred at 4 HPI. Upregulated genes belong to cellular processes, macromolecular metabolism, and transport, whereas downregulated genes seem to be associated mostly with regulatory processes (Dataset S07). Various studies have shown that the induction of the plant cell secretory pathway is relevant for the trafficking of molecules involved in the interaction between plants and microbes (Wang and Dong 2011). At 24 HPI, O157:H7 downregulated genes in functional categories associated with response to abiotic stimulus and circadian rhythm. Only two GO terms were identified as significantly represented in the upregulated gene dataset (Dataset S07).

STm 14028s modulated process. Interestingly, the only GO terms found to be enriched in the STm 14028s-4 HPI dataset are associated with RNA processing and gene expression, and these represented downregulated genes only. At 24 HPI, STm 14028s upregulated genes associated with cell wall modifications, hormone responses, and defense responses. The overall higher induction of genes related with defense response in Arabidopsis

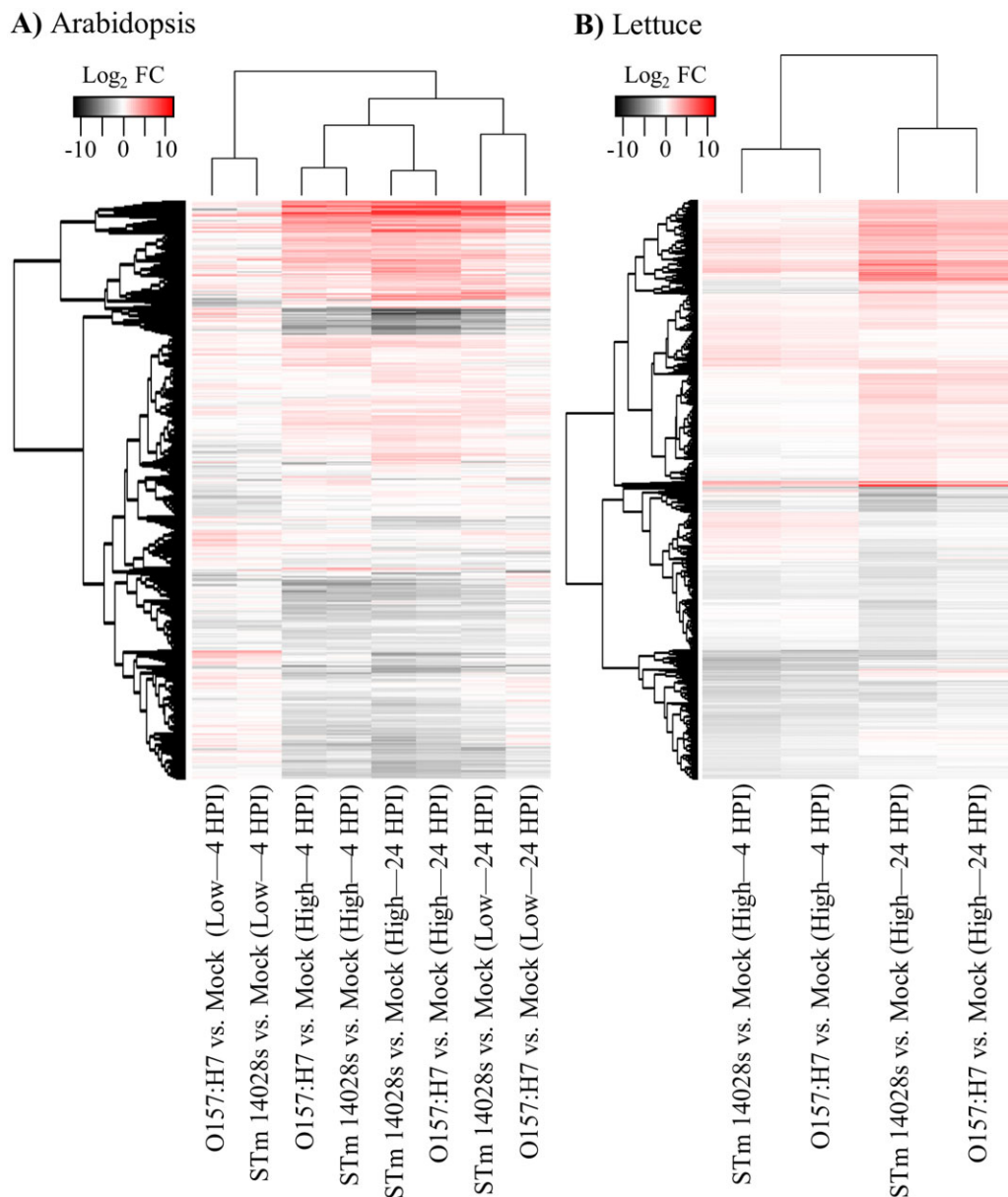


Figure 2 Hierarchical clustering analysis of differentially expressed genes (DEGs) in Arabidopsis (A) and lettuce (B) leaves at 4 and 24 h post inoculation (HPI) with low (5×10^6 CFU/ml) or high (1×10^9 CFU/ml) inoculum concentration of *Escherichia coli* O157:H7 and *Salmonella enterica* Typhimurium 14028s. Clustering was conducted using the heatmap.2 R package with default analysis settings. All DEGs were used as input for the hierarchical clustering analysis (7112 Arabidopsis genes and 7470 lettuce genes) and are listed in Dataset S03. FC, fold change.

after inoculation with STm 14028s than O157:H7 (Figure 4 and Supplementary Figure S6) is correlated with the significant decline of STm 14028s population in the apoplast over time as compared to that of O157:H7 (Figure 1A). In addition, at this later time point, genes downregulated by STm 14028s are associated with response to light and photosynthesis (Dataset S07), possibly because of heightened defense response.

Effects of increased bacterial population on the Arabidopsis transcriptome

Transcriptomic studies of plant responses during exposure to human pathogenic bacteria have been conducted under various experimental procedures and conditions. Although it is possible to use a very low inoculum concentration, such as 200 CFU/plant to inoculate *M. truncatula* seedlings (Jayaraman et al. 2014), a much higher inoculation dose is required for whole tissue

transcriptomic analysis so that all plant cells are exposed to a uniform number of bacterial cells (Katagiri et al. 2002). Previous microarray-based studies were performed with 14-day-old Col-0 seedlings submerged in liquid medium containing STm 14028s or its *prgH*- mutant at a final concentration of 1.7×10^8 and 2×10^8 CFU/ml, respectively (Schikora et al. 2011; Garcia et al. 2014). Thilmony et al. (2006) vacuum-infiltrated 4-week-old Col-0 plants with 1×10^8 CFU/ml of O157:H7 or its *fliC* mutant. However, these conditions would still not capture the bacterial transcriptomic for simultaneous analyses even with the latest Illumina technology. Thus, we sought to determine to what extent the inoculation dosage (5×10^6 or 1×10^9 CFU/ml) affects the plant transcriptome and aimed to analyze the bacterial metabolic changes in *planta*.

Arabidopsis leaves exposed to a high bacterial concentration exhibited an increase in both the number of total DEGs (Table 1)

TABLE 1. Number of significantly differentially expressed genes (DEGs) in the plant (*Arabidopsis* and lettuce) and bacteria (*Escherichia coli* O157:H7 and *Salmonella enterica* ser. Typhimurium 14028s) at 4 and 24 hours post inoculation (HPI), as well as in the bacterium inoculum. Putative orthologs of lettuce DEGs were identified in *Arabidopsis* as reported by Reyes-Chin-Wo et al. 2017. Modulated genes identified with each comparison are listed in Dataset S01.

Inoculum concentration	Genome	Comparison	Induced genes	Repressed genes	Total DEGs
5×10^6 CFU/ml	<i>Arabidopsis</i>	O157:H7 vs mock (4 HPI)	880	1443	2323
		O157:H7 vs mock (24 HPI)	523	482	1005
		STm 14028s vs mock (4 HPI)	136	623	759
		STm 14028s vs mock (24 HPI)	1470	1619	3089
1×10^9 CFU/ml	<i>Arabidopsis</i>	O157:H7 vs mock (4 HPI)	2176	2200	4376
		O157:H7 vs mock (24 HPI)	2523	2294	4817
		STm 14028s vs mock (4 HPI)	2327	1918	4245
		STm 14028s vs mock (24 HPI)	2928	2810	5738
	O157:H7	4 HPI vs inoculum	781	1379	2160
		24 HPI vs 4 HPI	60	60	120
	STm 14028s	4 HPI vs inoculum	526	2041	2567
		24 HPI vs 4 HPI	175	59	234
1×10^9 CFU/ml	Lettuce	O157:H7 vs mock (4 HPI)	691	999	1690
		O157:H7 vs mock (24 HPI)	2119	566	2685
		STm 14028s vs mock (4 HPI)	1502	1859	3361
		STm 14028s vs mock (24 HPI)	3124	2240	5364
	Arabidopsis (orthologs of lettuce DEGs)	O157:H7 vs mock (4 HPI)	446	730	1176
		O157:H7 vs mock (24 HPI)	1206	411	1617
		STm 14028s vs mock (4 HPI)	1042	1377	2419
		STm 14028s vs mock (24 HPI)	1928	1770	3698
	O157:H7	4 HPI vs inoculum	372	234	606
		24 HPI vs 4 HPI	63	101	164
	STm 14028s	4 HPI vs inoculum	249	526	775
		24 HPI vs 4 HPI	143	92	235

and the overall intensity of transcriptional regulation (Figure 2A). High-level inoculation also resulted in a similar response of *Arabidopsis* to both O157:H7 and STm 14028s when compared to plants inoculated with the low inoculum concentration (Figure 2A). The effect of different inoculum concentrations in the overall transcriptomic changes of *Arabidopsis* was less prominent at 24 HPI compared with that at 4 HPI (Figure 2A). The hierarchical analysis clustered the 24 HPI-low inoculum treatments in a subgroup closer to all high inoculum treatments than to the 4 HPI-low inoculum treatments (Figure 2A), suggesting that high inoculum induced faster and stronger response as expected. This is particularly evident in *Arabidopsis* leaves inoculated with low STm 14028s concentrations at 24 HPI that exhibited a pattern of gene transcriptional modulation very similar to those of samples from high inoculum concentration treatments (Figure 2A).

We next determined the extent of overlap between *Arabidopsis* DEGs identified in leaves exposed to the two inoculum concentrations. Overall, the proportion of DEGs shared between the two inoculation levels is low at 4 HPI for both bacteria, where approximately 10% of the DEGs in the low inoculum dataset is also present in the high inoculum dataset. However, at 24 HPI, more than 30 and 55% of DEGs in the low inoculum dataset is also present in the high inoculum dataset obtained from O157:H7 and STm 14028s, respectively (Supplementary Figure S7, C and D; Dataset S06).

To understand the biological function of genes commonly or uniquely differentially expressed between low and high inoculum concentration treatments, we conducted a GO enrichment analysis of each overlapping dataset (Dataset S09). This analysis showed that among the different datasets, most of the GO terms enriched among downregulated genes were related to photosynthesis and primary metabolism, while those enriched among upregulated genes were generally associated with stress response. The biological processes affected by different bacterial inoculum concentrations were similar; however, there was a

relevant increment in the number of significantly DEGs belonging to primary and secondary metabolism (Figure 3; Dataset S04), as well as to biotic stress (Figure 4; Dataset S05) in *Arabidopsis* inoculated with the high inoculum concentration compared to those inoculated with the low inoculum concentration.

Taken together, these findings suggest that, with the purpose of identifying plant metabolic processes affected by O157:H7 and STm 14028s, high inoculation dosages are appropriate and provide the advantage of studying simultaneous changes in the bacterial transcriptomic profiles.

Overlap between transcriptional profiles of *Arabidopsis* and lettuce exposed to O157:H7 and STm 14028s

Due to the relevance of lettuce for the market of fresh vegetables (Lucier and Parr 2020) and its frequent association with food safety incidents (Turner et al. 2019; Marshall et al. 2020), we analyzed changes in the transcriptomic profiles of leaves of the lettuce cultivar Salinas (Reyes-Chin-Wo et al. 2017) after exposure to either STm 14028s or O157:H7. With the exception of 24 HPI with STm 14028s, fewer lettuce genes were modulated by these bacteria as compared to those of *Arabidopsis* (Table 1). Furthermore, hierarchical clustering analysis of DEGs showed that, although datasets formed two clusters by time point, STm 14028s seems to induce stronger changes than O157:H7 indicated by the darker color at both time points (Figure 2B; Dataset S03).

The initial analyses described above were conducted with the original lettuce genes to call significant modulation (Dataset S01) and enriched GO terms using the Blast2GO software (Dataset S02). However, translating the lettuce genes into their corresponding *Arabidopsis* orthologs (Dataset S01) followed by functional annotation with the PANTHER14.1 tool proved to be more informative (Dataset S02). On average, 3.5 and 4.6 times more enriched GO terms were detected with PANTHER14.1 than Blast2GO at 4 and 24 HPI, respectively (Dataset S02), possibly due

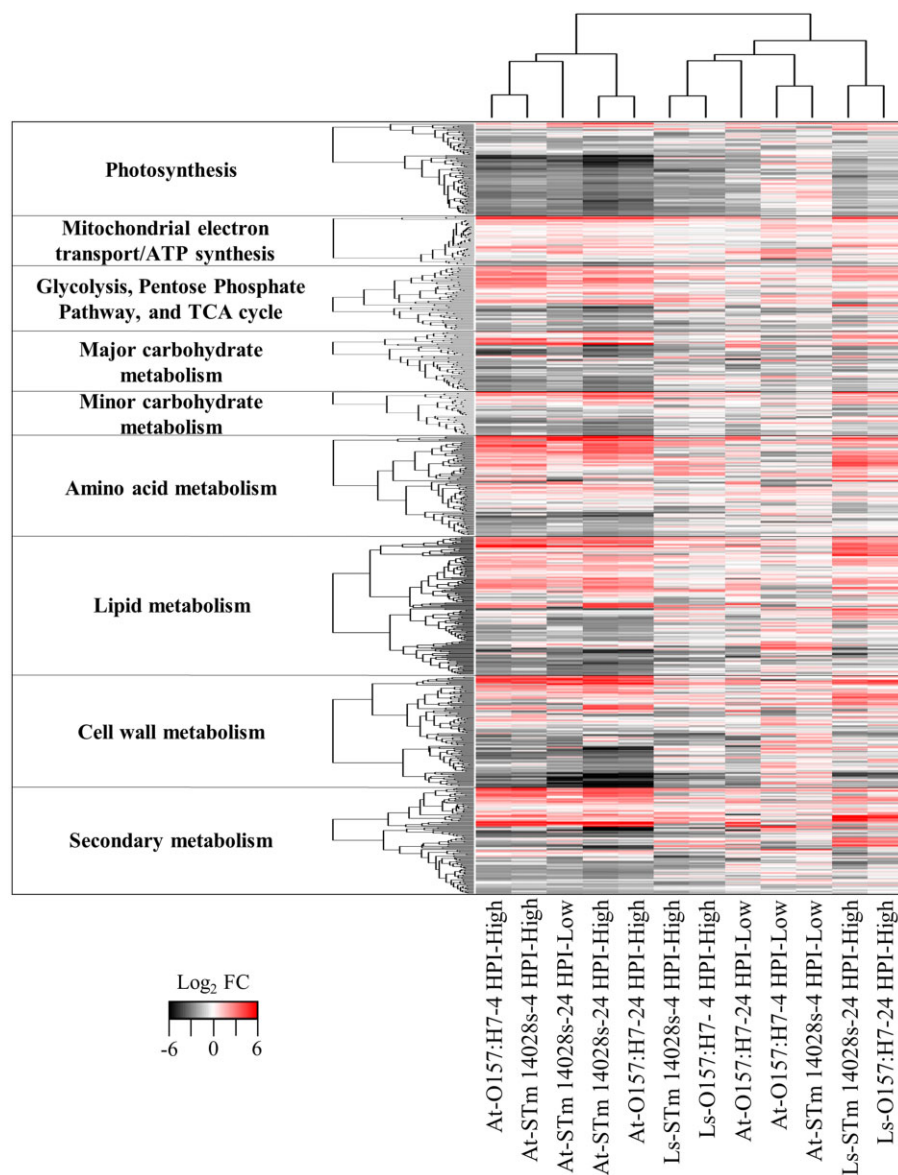


Figure 3 Hierarchical clustering analysis of differentially expressed genes (DEGs) involved in primary and secondary metabolism of Arabidopsis (At) and lettuce (Ls) at 4 and 24 h post inoculation (HPI) with a low (5×10^6 CFU/ml) or high (1×10^9 CFU/ml) inoculum concentration of *Escherichia coli* O157:H7 and *Salmonella enterica* Typhimurium 14028s. Clustering was conducted using the heatmap.2 R package with default analysis settings. The list of DEGs is described in Dataset S04. FC = fold change.

to the lower level of functional annotation of the lettuce genome as compared to the Arabidopsis genome (Reyes-Chin-Wo et al. 2017). It is important to note that an Arabidopsis ortholog could not be assigned to 23% of all lettuce genes (Reyes-Chin-Wo et al. 2017) and they were not included in further analyses. However, the conversion of lettuce genes to orthologous Arabidopsis genes provided two advantages, the increased functional annotation and the comparison of the bacterial-induced transcriptomic response between the two plant species as described below.

The number of lettuce genes modulated by STm 14028s was considerably larger than the number of O157:H7-modulated genes in comparison with the mock control (Table 1). This is in stark contrast with Arabidopsis, where both bacteria modulated a similar number of genes and the number of genes modulated was greater than that in lettuce (Table 1), suggesting distinct plant-bacterium interactions. These differences might be influenced by the total number of genes in the genome of each plant

species: 27,655 in Arabidopsis (Cheng et al. 2017) and 38,919 in lettuce (Reyes-Chin-Wo et al. 2017). In addition, evolutionary forces (i.e., plant domestication and bacterial adaptation to different environments) may also play a role in the differential interaction between these organisms.

By identifying the putative Arabidopsis orthologs of lettuce DEGs (Dataset S01), it was possible to use them as input to reconstruct the major metabolic pathways and biotic stress response maps. This analysis again showed that STm 14028s modulates more genes than O157:H7 in both time points and most genes are downregulated at 4 HPI, whereas most genes are upregulated at 24 HPI (Supplementary Figures S8 and S9).

After identifying the DEGs in each plant species (bacterium versus mock control) at the two time points (Dataset S01), we conducted a pairwise comparison between different datasets. Overall, a larger overlap between the two plant species was observed in STm 14028s-modulated genes than O157:H7-modulated

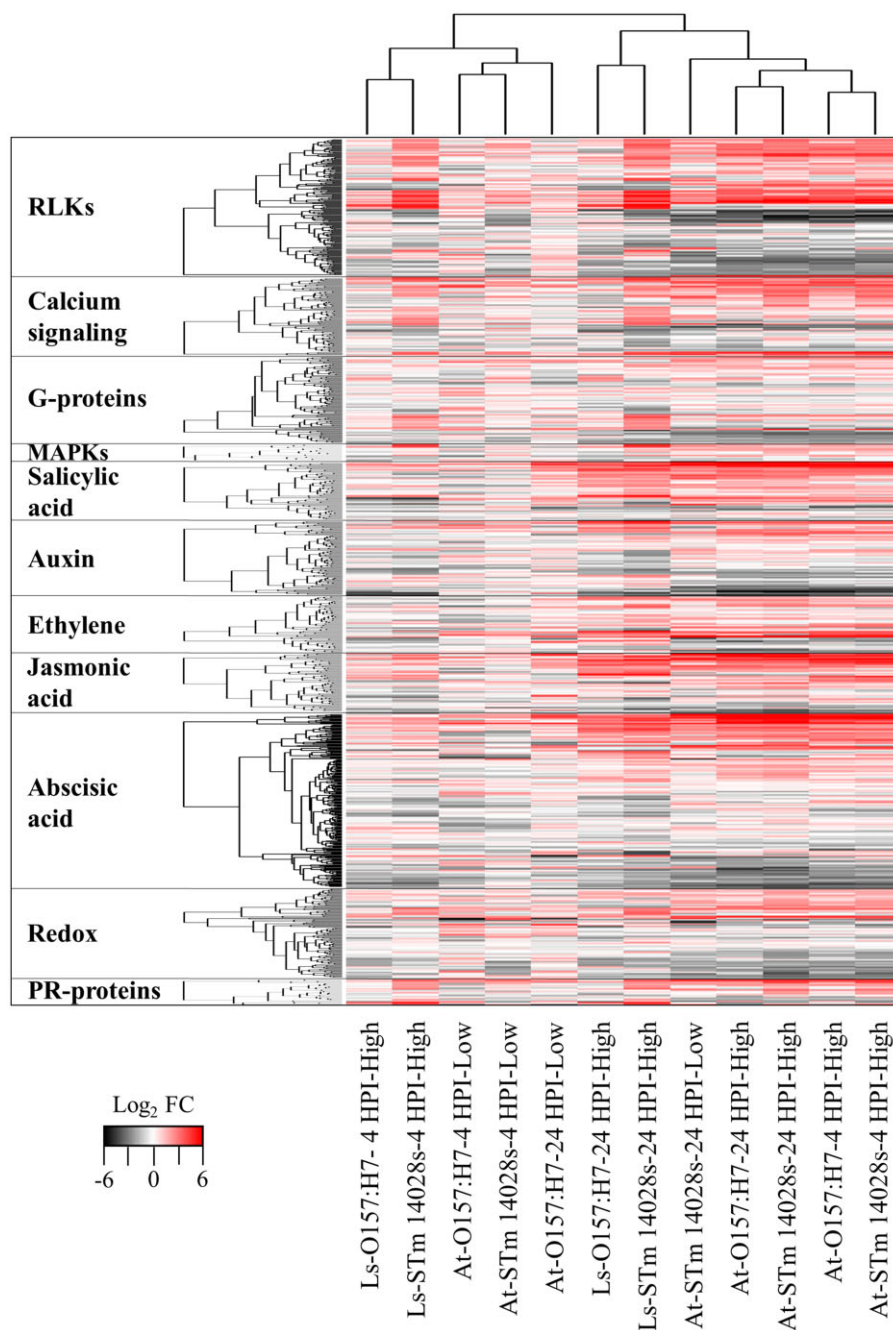


Figure 4 Hierarchical clustering analysis of differentially expressed genes (DEGs) involved in biotic stress responses of Arabidopsis (At) and lettuce (Ls) at 4 and 24 h post inoculation (HPI) with a low (5×10^6 CFU/ml) or high (1×10^9 CFU/ml) inoculum concentration of *Escherichia coli* O157:H7 and *Salmonella enterica* Typhimurium 14028s. Clustering was conducted using the heatmap.2 R package with default analysis settings. The list of DEG is described in Dataset S05. RLKs, receptor-like kinases; MAPKs, mitogen-activated protein kinases; PR, pathogenicity related; FC, fold change.

genes (Supplementary Figure S7, E and F; Dataset S06). Furthermore, the number of DEGs shared between the two time points was two or more times larger in Arabidopsis than lettuce (Supplementary Figure S7, E and F), suggesting that transcriptional changes in Arabidopsis last longer than in lettuce. Next, we analyzed the functional categories of DEGs that are shared by or unique to each plant species (Dataset S10).

Functional categories shared by both Arabidopsis and lettuce in response to human pathogens

Genes that were downregulated at 4 HPI in both plant species enriched GO terms involving photosynthesis (Figure 3; Dataset

S04) and circadian rhythm after inoculation with O157:H7 or STm 14028s. The repression of photosynthesis contributes to the growth–defense tradeoffs during plant–pathogen interactions (Huot et al. 2014). Interestingly, both biological processes, photosynthesis and circadian rhythm, were largely repressed in lettuce cultivar Salinas inoculated with *B. cinerea* (De Cremer et al. 2013). The circadian clock in plants participates in the regulation of growth and development (i.e., photosynthesis, stomatal movement, flowering, and senescence) and responses against abiotic and biotic stressors (Srivastava et al. 2019).

At 24 HPI, repressed genes shared by both plant species were associated with different biological processes depending on the

human pathogenic bacteria. In the case of leaves inoculated with STm 14028s, all repressed genes at 24 HPI in both plant species were associated with photosynthesis (Figure 3; Dataset S04). In contrast, genes commonly downregulated in *Arabidopsis* and lettuce at 24 HPI with O157:H7 were related with growth and development (i.e., pattern specification process, response to auxin, and shoot system development) (Dataset S10).

Genes commonly upregulated in both plant species at 4 and 24 HPI with either STm 14028s or O157:H7 belong to the overrepresented GO categories related to plant defense responses (Figure 4; Dataset S05). However, the overall upregulation of genes associated with biotic stress in *Arabidopsis* leaves was higher compared to that observed in lettuce (Figure 4; Dataset S05). In addition, at 4 HPI, other biological processes, such as those represented by the GO terms *de novo* protein folding, endoplasmic reticulum unfolded protein response, and response to heat, were overrepresented by DEGs present in both plant species after inoculation with O157:H7 and STm 14028s.

Functional categories unique to lettuce in response to human pathogens

A biological process only induced in lettuce at 4 HPI is associated with ribosome biology and translation, such as the GO terms maturation of LSU- and SSU-rRNA from tricistronic rRNA transcript, ribosomal large subunit assembly, and translational elongation. Additionally, the GO term “phenylpropanoid biosynthetic process,” which is associated with chemical defenses against pathogens (Dixon et al. 2002), was only enriched among induced DEGs in lettuce, but not in *Arabidopsis*, after inoculation with STm 14028s or O157:H7 (Dataset S10). Similarly, one of the most relevant transcriptional changes caused by the inoculation with the necrotrophic pathogen *Botrytis cinerea* in 5-week-old lettuce cv. Salinas plants grown in soil was the induction of the phenylpropanoid pathway (De Cremer et al. 2013). Regulation of this pathway may be associated with lettuce response to a wide range of microbes.

The GO term “ethylene-activated signaling pathway” was specifically overrepresented among upregulated lettuce genes at 24 HPI with STm 14028s (Dataset S10). Various genes involved in the ethylene signaling pathway were also detected in the lettuce cv. Tizian after inoculation with STm 14028s (Jechalke et al. 2019), suggesting that ethylene response in lettuce may be specific to STm isolates.

Interestingly, the GO term “regulation of stomatal movement” was enriched only among repressed genes in lettuce at 4 HPI with STm 14028s (Dataset S10). Previously, we have shown that the stomatal closure in lettuce is sustained for several hours after inoculation with O157:H7; however, at 4 HPI leaves inoculated with STm strains SL1344 and 14028s exhibit a reopening of the stomatal pore (Roy et al. 2013; Montano et al. 2020). Although these STm strains regulate stomatal movement in *Arabidopsis* (Roy et al. 2013), this functional category was not enriched in *Arabidopsis* DEG datasets, suggesting that this response may be more prominent in lettuce than in *Arabidopsis*.

Overall, we observed significant differences between plant species in the modulation of genes within the broad GO term “biological functions,” in addition to a few specific GO terms exclusively enriched in *Arabidopsis* or lettuce samples after inoculation with the human pathogenic bacteria O157:H7 and STm 14028s.

Bacterial responses to the *Arabidopsis* and lettuce apoplast environments

To assess potential metabolic changes that occur in the bacterial cells when they transitioned from the inoculum environment to the leaf apoplast, we compared the bacterial transcriptomic profiles in the inoculum with that at 4 HPI into the leaf apoplast (4 HPI vs inoculum; Table 1). In addition, subsequent changes in bacterial gene expression once in the apoplast were also assessed (24 HPI vs 4 HPI; Table 1).

Overall, both O157:H7 and STm 14028s exhibited a substantially larger transcription modulation at 4 HPI in the leaf environment compared to 24 HPI, both in number of DEGs (Table 1) and the extent of FC (Supplementary Figure S10; Dataset S11) in both plant species. This suggests that the metabolic changes taking place during the first hours in the leaf are crucial for the adaptation of the bacteria to the new environment and that most of these changes are sustained and only small readjustments are made in the subsequent 20h. These observations were expected considering the change from a nutritional rich media to a relatively nutritional limited environment, the leaf apoplast. Furthermore, bacteria exposed to the apoplastic environment of *Arabidopsis* exhibited larger changes in the transcription of genes as compared to bacteria infiltrated into lettuce leaves, especially at 4 HPI (Supplementary Figure S10), suggesting that bacterial interactions with *Arabidopsis* are initially more intense than that with lettuce. These differences correlate with the overall stronger transcriptomic adjustments induced by O157:H7 and STm 14028s in *Arabidopsis* than in lettuce (Table 1; Figure 2; Dataset S03) and with the overall larger population of O157:H7 and STm 14028s during the first 24 HPI in lettuce compared with *Arabidopsis* (Figure 1).

Overlap analysis of bacterial DEG datasets in *Arabidopsis* and lettuce

Cellular metabolism in *Salmonella* and *E. coli* is complex and adaptable to different nutritional environments (AbuOun et al. 2009). Accordingly, we observed some commonalities and uniqueness in the transcriptome modification of both O157:H7 and STm 14028s when comparing the lettuce and *Arabidopsis* environments (Supplementary Figure S7, G and H; Dataset S06). To analyze the biological functionality of specific and shared transcriptomic changes of STm 14028s and O157:H7, we conducted a KEGG enrichment analysis through the hypergeometric test (Figure 5). This analysis revealed that, at 4 HPI, main metabolic pathways were significantly enriched depending upon plant-bacterium combinations (Figure 5).

Furthermore, as genes associated with specific metabolic processes are organized in operons and gene clusters in the bacterial genome, we assessed whether multiple genes in these regions were co-regulated (Supplementary Figure S10; Dataset S11) and created metabolic maps with predicted proteins encoded by the DEGs (Supplementary Figure S11; Dataset S12).

Both O157:H7 and STm 14028s exhibited an upregulation of the genes of the phage shock protein *psp* operon at 24 HPI in both lettuce and *Arabidopsis* (Figures 6 and 7). The phage shock protein system is synthesized not only in response to phage infection, but also under multiple stressors (Flores-Kim and Darwin 2016). This seems to be a common bacterial response to the plant environment, as one of the largest group of genes upregulated in *E. coli* K-12 after spray inoculation on lettuce leaves included the *psp* operon (Fink et al. 2012).

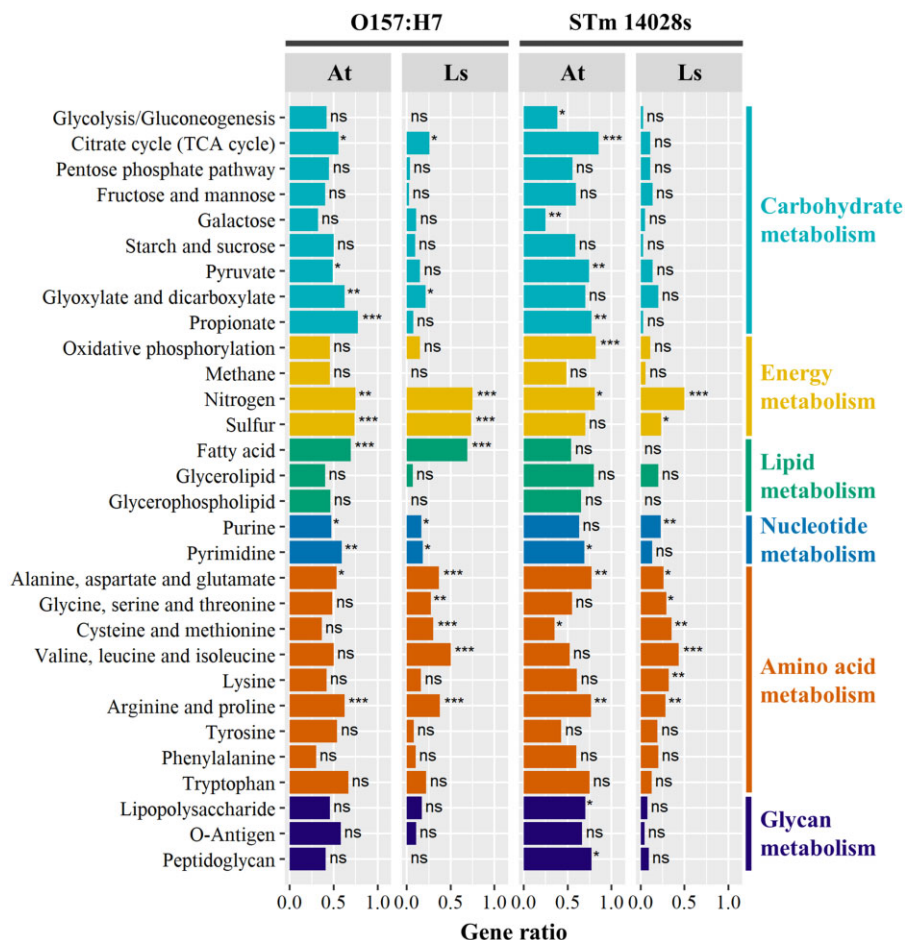


Figure 5 KEGG pathway enrichment analysis of genes differentially expressed by *Escherichia coli* O157:H7 and *Salmonella enterica* ser. Typhimurium 14028s after 4 h of inoculation in *Arabidopsis thaliana* (At) and lettuce (Ls = *Lactuca sativa* cv. Salinas). Gene ratio corresponds to the number of differentially expressed genes mapped to a KEGG pathway divided by the total number of genes comprising that KEGG pathway. To map the genes to the metabolic pathways, the protein sequences of the corresponding annotated genome were used to obtain the KEGG protein IDs using the KofamKOALA BLAST tool (<https://www.genome.jp/tools/kofamkoala/>). Protein sequences with an E-value lower than $10E^{-5}$ (listed in Dataset S12) were used as input for the KEGG Mapper Reconstruct Pathway tool (https://www.kegg.jp/kegg/tool/map_pathway.html). Enrichment analysis was conducted with the hypergeometric test (ns = P-value ≥ 0.5 ; *P-value < 0.5 ; **P-value < 0.01 ; ***P-value < 0.001).

We also observed multiple gene clusters that were modulated in O157:H7 and/or STm 14028s in a plant-dependent manner (Dataset S11), which are discussed below.

Influence of the plant species on the expression of O157:H7 operons

Operons modulated in both plant species. O157:H7 exhibited a strong regulation of nitrogen metabolism during exposure to the leaf apoplast (Figure 5). For example, the four highest upregulated genes in both plant species are part of the seven-gene operon *rutABCDEFG* that encodes a pathway to derive nitrogen from the degradation of pyrimidines (Figure 6; Parales and Ingraham 2010). O157:H7 also stimulated the expression of the *glnALG* operon and the nitrogen regulatory protein P-II 1 (XF37_18635; Dataset S11) that is involved in response to nitrogen starvation (Javelle and Merrick 2005), as well as the induction of the *trp* operon that controls tryptophan biosynthesis under changes in the nutritional environment (Figure 6; Yanofsky and Horn 1994). Moreover, O157:H7 upregulated the complete *liv* (leucine/isoleucine/valine transport system) operon (Figure 6; Bhagwat et al. 1997). These results reveal a common metabolic adaptation of O157:H7 to the nitrogen environment of the leaf apoplast of lettuce and Arabidopsis.

Sulfur metabolism was enriched in both plant species in O157:H7 (Figure 5), upregulating both *tauABCD* and *ssuEADCB* operons (Figure 6). The gene clusters *tauABCD* and *ssuEADCB* are required for the bacterial utilization of taurine and alkanesulfonates as sulfur sources and are expressed only under conditions of sulfate or cysteine starvation (Eichhorn et al. 2000). The expression of these gene clusters suggests a potential sulfate or cysteine limitation in Arabidopsis and lettuce leaves for the metabolism of O157:H7.

Operons uniquely modulated in Arabidopsis. A much larger number of O157:H7 operons and metabolic pathways were modulated in the transition to Arabidopsis than lettuce (i.e., 4 HPI vs inoculum; Figure 5; Dataset S11). The *lsr* (*luxS* regulated) operon was induced in O157:H7 (Figure 6). This operon is responsible of the uptake and processing of the quorum sensing autoinducer-2 (AI-2) molecule that controls genes involved in virulence factors (Pereira et al. 2013). Notably, operons involved in bacterial virulence mechanisms were significantly downregulated, including the locus of enterocyte effacement (*lee1-7*) (Gaytán et al. 2016), the type three secretion system apparatus and effectors gene cluster (TTSS-2; Zhou et al. 2014), the chemotaxis and motility (*che-mot*) operon (Ditty et al. 1998), the flagellar (*flg* and *fli*; Liu and Ochman 2007) and fimbrial (*fim*) formation operons, and the CA gene

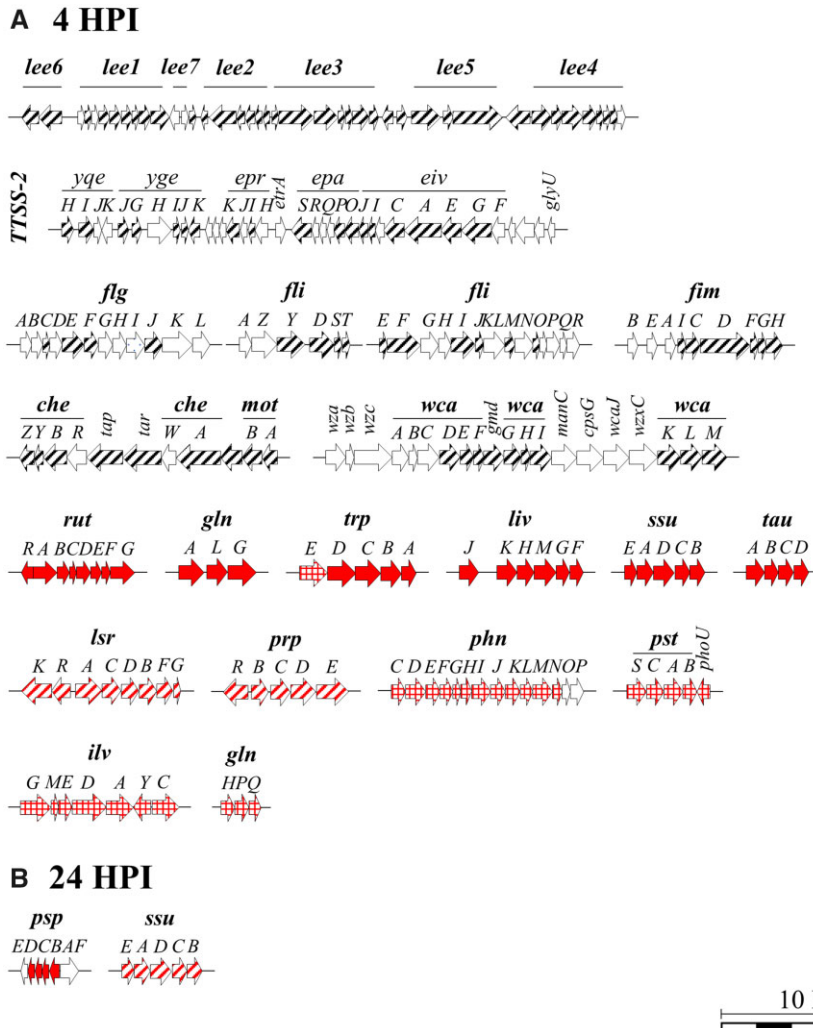


Figure 6 Major operons and gene clusters significantly modulated in *Escherichia coli* O157:H7 at 4 h (A) and 24 h (B) post inoculation (HPI). Locus of enterocyte effacement (*lee1-7*), type three secretion system 2 (TTSS-2), flagella (*flg* and *fli*), fimbria (*fim*), chemotaxis and motility (*che-mot*), colanic acid (*wca*), Rut pathway (*rut*), glutamine synthase (*glnALG*), tryptophan (*trp*), leucine, isoleucine, and valine transport system (*liv*), sulfonate-sulfur utilization (*ssu*), taurine utilization (*tau*), luxS-mediated quorum sensing (*lsr*), propionate (*prp*), organophosphonate utilization (*phn*), phosphate transporter (*pst*), isoleucine and valine biosynthetic pathway (*ilv*), glutamine transporter (*glnHPQ*), and phage shock proteins (*psp*). Genes differentially expressed in lettuce only (squared), Arabidopsis only (striped), and both lettuce and Arabidopsis (filled) are depicted within each operon and gene cluster. Genes colored in red, black, or white indicate upregulation, downregulation, or not differentially expressed, respectively. Schematic representation of operons and gene clusters was created based on the Ensembl Bacteria (<https://bacteria.ensembl.org/index.html>) genome browser. Description of the operons can be found in Dataset S11.

cluster (*wca*; Wu et al. 2019) (Figure 6). Interestingly, virulence factors of O157:H7 (i.e., LEE and TTSS) have shown a positive role in the colonization of spinach after surface inoculation (Saldaña et al. 2011), which suggest that the participation of these elements on plant colonization by O157:H7 might be dependent on experimental factors, such as inoculation method.

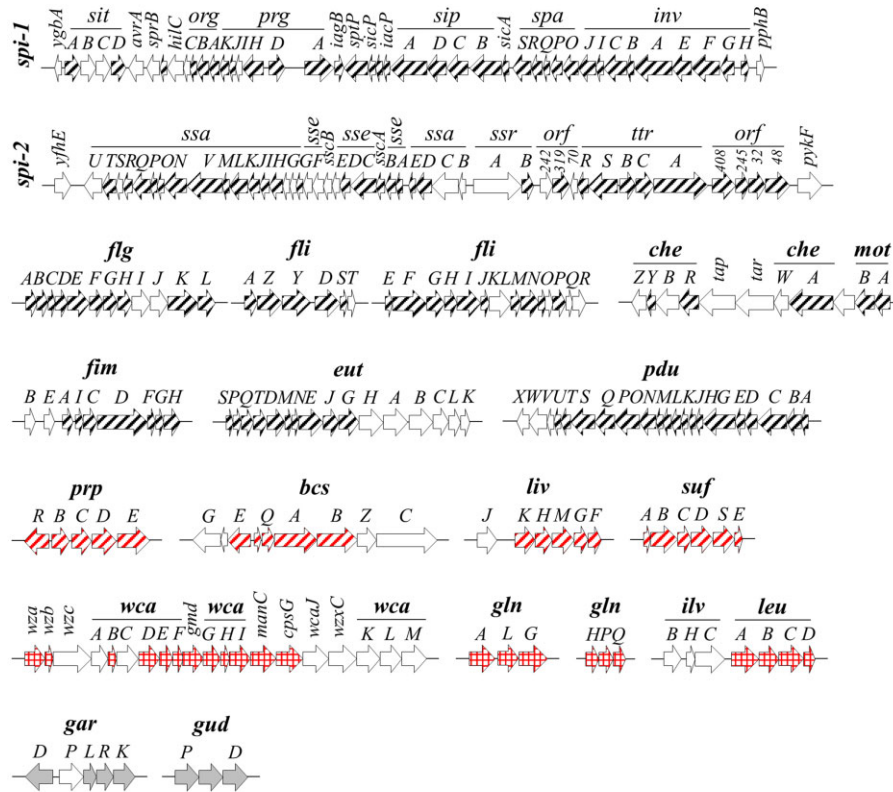
Significant repression of genes related to energy generation occurred in O157:H7 (Figure 5 and Supplementary Figure S12, A and B). *E. coli* and related enterobacteria can couple the reduction of nitrate and nitrite to ammonium to energy-conserving respiratory electron transport systems, which occurs in many electron-rich environments such as the human gastrointestinal tract (Cole and Richardson 2008). In Arabidopsis, O157:H7 repressed the whole nitrate reductase-cytochrome c maturation (*nap-ccm*) locus (Stewart et al. 2002) and the respiratory nitrite reductase gene cluster *nrf*ABCDEFG (Wang and Gunsalus 2000; Supplementary Figure S12, A and B). Similarly, after spray inoculation on lettuce leaves, *E. coli* K-12 largely downregulated processes involved in

energy metabolism, including nitrate reductase genes (Fink et al. 2012).

Genes involved in the utilization of certain carbon sources were significantly modulated only in Arabidopsis (Figure 5). For instance, O157:H7 induced the propionate *prp*RBCDE operon at 4 HPI (Figures 5 and 6), which metabolizes propionate via the 2-methylcitric acid cycle that yields pyruvate and succinate (Horswill and Escalante-Semerena 2001). Propionate is among the most abundant nutrients present in the colon and it is degraded by several members of the gut microbiota (Rivera-Chávez and Bäuml 2015).

Operons uniquely modulated in lettuce. O157:H7 genes with the highest Log₂ FC were those in the *phn* operon (Figure 6; Dataset S11), which is responsible for organophosphonate utilization (Jochimsen et al. 2011). In addition, O157:H7 induced the genes of the high-affinity phosphate transport system *pst*SCAB-*phoU* operon (Figure 6) and the two-component regulatory mechanism proteins PhoR (XF37_18915) and PhoB (XF37_18920;

A 4 HPI



B 24 HPI

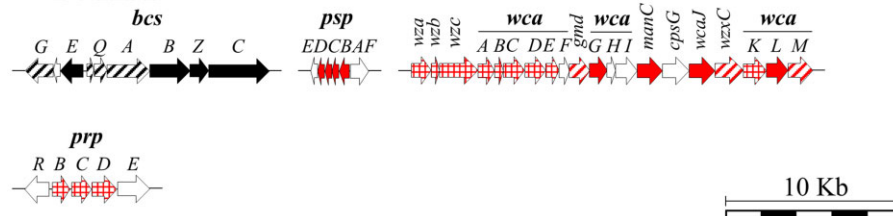


Figure 7 Major operons and gene clusters significantly modulated in *Salmonella enterica* ser. Typhimurium 14028s at 4 h (A) and 24 h (B) post inoculation (HPI). *Salmonella* pathogenicity island-1 (*spi-1*) and -2 (*spi-2*), flagella (*flg* and *fli*), chemotaxis and motility (*che-mot*), fimbria (*fim*), ethanolamine (*eut*), propanediol (*pdu*), propionate (*prp*), bacterial cellulose synthase (*bcs*), leucine, isoleucine, and valine transport system (*liv*), sulfur formation system (*suf*), colanic acid (*wca*), glutamine synthase (*glnALG*), glutamine transporter (*glnHPQ*), leucine biosynthesis (*ilv-leu*), D-galactarate (*gar*), D-glucarate (*gud*), and phage shock proteins (*psp*). Genes differentially expressed in lettuce only (squared), Arabidopsis only (striped), and both lettuce and Arabidopsis (filled) are depicted within each operon and gene cluster. Genes colored in red, black, or white indicate upregulation, downregulation, or not differentially expressed, respectively. Genes colored in gray showed opposite expression patterns in each plant species (operons *gar* and *gud* were induced in lettuce and repressed in Arabidopsis). Schematic representation of operons and gene clusters was created based on the Ensembl Bacteria (<https://bacteria.ensembl.org/index.html>) genome browser. Description of the operons can be found in Dataset S11.

Dataset S11), which are activated during phosphate starvation to regulate phosphate homeostasis (Gardner et al. 2014). Furthermore, various pathways involved in amino acid metabolism were exclusively significantly enriched by O157:H7 in lettuce (Figure 5). The *ilv* operon, which encodes enzymes forming the isoleucine and valine biosynthetic pathway (Wechsler and Adelberg 1969), and the glutamine ABC transporter (*glnHPQ*) operon were only induced in O157:H7 inoculated into lettuce (Figure 6; Dataset S11). These findings suggest plant specificity in substrate utilization by O157:H7. A similar observation has been reported in other plant systems where genes associated with metabolic responses were differentially modulated during O157:H7 growth in lettuce and spinach cell wall polysaccharides, spinach leaf lysates, and root exudates (Crozier et al. 2016). The study conducted by Kyle et al. (2010) also showed a significant

modulation of various genes involved in the carbohydrate transport systems in O157:H7 when growing in lettuce leaf lysates, revealing the bacterial availability to use carbohydrates released from injured plant cells.

Influence of the plant species on the expression of STm 14028s operons

Operons modulated in both plant species. Certain operons involved in carbon and nitrogen metabolism were commonly modulated in lettuce and Arabidopsis by STm 14028s (Figure 5; Dataset S11). Similar to O157:H7, STm 14028s induced the propionate *prpRBCDE* operon at 4 HPI in Arabidopsis and at 24 HPI in lettuce (Figure 7), which metabolizes propionate via the 2-methylcitric acid cycle that yields pyruvate and succinate (Horswill and Escalante-Semerena 2001). In addition, genes

belonging to the operons *gar* and *gud*, responsible of the degradation and utilization of D-galactarate and D-glucarate as a source of carbon (Monterrubio et al. 2000), were repressed by STm 14028s in Arabidopsis while induced in lettuce at 4 HPI (Figure 7). Furthermore, the expression of the two genes encoding glutamate synthase (MC58_20705 and MC58_20710; Dataset S11), an enzyme also involved in the bacterial assimilation of nitrogen (van Heeswijk et al. 2013), was repressed in Arabidopsis and induced in lettuce.

Genes within operons involved in biofilm formation were significantly modulated. For instance, STm 14028s induced genes of the CA (*wca*) gene cluster in both plants at 24 HPI, whereas induction of these genes started at 4 HPI in lettuce (Figure 7). In addition, this bacterium repressed genes of the bacterial cellulose synthesis (*bcs*) operon (Römling and Galperi 2015) in both plant species at 24 HPI (Figure 7). The role in attachment and persistence of genes involved in the formation of the extracellular matrix has been studied in multiple plant species (Yaron and Römling 2014). For instance, mutants of *S. enterica* ser. Enteritidis with deletions in the *bcsA* or *wcaD* genes exhibited a significant reduction in the attachment to and survival on alfalfa sprouts (Barak et al. 2007).

Operons uniquely modulated in Arabidopsis. In Arabidopsis, STm 14028s repressed several genes comprising the *Salmonella* pathogenicity islands 1 and 2 (SPI-1 and SPI-2; Figure 7), which enable the efficient penetration of the intestinal epithelium (Phoebe et al. 2001; Figueira and Holden 2012). Similar to O157:H7, we detected repression of multiple STm 14028s genes comprising the flagella (*flg* and *fli*; Liu and Ochman 2007) and the chemotaxis gene clusters (*che-mot*; Ditty et al. 1998), together with genes encoding fimbrial (*fim*) proteins (Figure 7). Zarkani et al. (2020) also reported that STm 14028s generally repressed the flagellin production during the colonization of tomato plants.

Genes involved in the utilization of certain carbon sources and the transport of amino acids were also significantly modulated only in Arabidopsis (Figure 5). Ethanolamine and 1,2-propanediol can be utilized by *S. enterica* as a sole carbon source by inducing, respectively, the ethanolamine (*eut*) and propanediol (*pdu*) utilization operons (Srikumar and Fuchs 2011). The genes most repressed by STm 14028s included 18 genes of the 23-gene *pdu* operon and various genes of the *eut* operon were repressed (Figure 7). Ethanolamine is an important source of carbon and/or nitrogen for pathogenic bacteria, it is particularly prevalent in the gastrointestinal tract, and it contributes to infection and colonization in the host (Rivera-Chávez and Bäumlér 2015; Kaval and Garsin 2018). Furthermore, STm 14028s upregulated most of the genes comprising the *liv* operon only in Arabidopsis (Figure 7).

Similar as in O157:H7, multiple genes involved in energy generation were repressed by STm 14028s (Figure 5 and Supplementary Figure S12, C and D). Energy production involves respiratory chains that mainly consist of dehydrogenases and terminal reductases or oxidases that are linked by quinones (Unden et al. 2014). STm 14028s downregulated 12 genes in Arabidopsis belonging to the NADH dehydrogenase A/B gene operon, the entire *atp* operon, which encodes for the bacterial F1F0-ATP synthase and includes the genes ATP synthase subunit IACB $\delta\alpha\gamma\beta\epsilon$ (Preiss et al. 2015), and the whole *frdABCD* operon, which encodes the fumarate reductase enzyme complex (Supplementary Figure S12A). A larger number of genes related to respiration were suppressed in STm 14028s than that in O157:H7 in Arabidopsis (Figure 5 and Supplementary Figure S12).

In Arabidopsis, STm 14028s stimulated the expression of multiple genes involved in response to oxidative stress such as flavin

mononucleotide (FMN)-dependent NADH-azoreductase (MC58_07180), glutaredoxin (MC58_10275), peroxidase (MC58_16865), alkyl hydroperoxide reductase (MC58_11560), and thioredoxin reductase (MC58_10035) (Dataset S11). In addition, the *sufABCDS*E operon that encodes the sulfur formation system stimulated under iron limitation and oxidative stress (Ayala-Castro et al. 2008) was induced (Figure 7). It has been suggested that the response of *Salmonella* ser. Newport to oxidative stress induced in tomato plants is crucial for the survival of bacteria in the plant environment (Ferelli et al. 2020).

Operons uniquely modulated in lettuce. Similar to O157:H7, STm 14028s induced the expression of the *glnALG* operon, in addition to stimulating the glutamine ABC transporter (*glnHPQ*) operon in lettuce (Figure 7). Glutamine synthetase is key for the bacterial assimilation of nitrogen and the *glnALG* operon, which encodes two nitrogen regulation proteins, NR(I) and NR(II) and a glutamine synthetase (van Heeswijk et al. 2013), is induced under limiting nitrogen sources (Ueno-Nishio et al. 1983). The two most upregulated genes by STm 14028s in lettuce were the ones encoding nitrogen regulatory protein P-II 1 (MC58_12240) and the ammonium transporter (MC58_12235; Dataset S11). Furthermore, the operon encoding the genes for the biosynthesis of leucine (*ilv-leu*), which is regulated in response to leucine availability (Grandoni et al. 1992), was induced only in lettuce (Figure 7; Dataset S11).

Altogether, these results indicate that STm 14028s and O157:H7 exhibit common and unique responses to the apoplast of lettuce and Arabidopsis leaves, which might have a role in the differential capacity of these human pathogenic bacteria to persist inside the leaf. Furthermore, these responses suggest the existence of specific modulation of their metabolism for survival in an environment that is substantially different from their natural niche, the gastrointestinal tract (Hirt 2020).

Conclusions

- I. The transcriptomic analyses enabled the discovery of common and specific modulation of biological processes in Arabidopsis and lettuce upon stimulation by STm 14028s or O157:H7 that are bacterial species- and time-dependent.
- II. Plant transcriptomic readjustments after infiltration with STm 14028s or O157:H7 are characterized by an overall downregulation of genes involved in photosynthesis and upregulation of genes associated to responses against biotic stressors. These results agree with the growth-defense tradeoffs commonly observed during plant-pathogen interactions.
- III. Human pathogenic bacteria cause more transcriptomic changes in Arabidopsis than in lettuce. This finding exposes the significant effect of plant genotypic variation in the interaction between the leaf and human pathogenic bacteria at the genome-wide level.
- IV. At 24 HPI, STm 14028s induces an overall larger modulation of transcription in lettuce and Arabidopsis as compared to that of O157:H7. A stronger stimulation of defense responses by STm 14028s than O157:H7 was observed, which was associated with a lower capability of STm 14028s to persist in the leaf apoplast than O157:H7, revealing a variation in the potential risk of contamination of leaves by different species of human pathogenic bacteria.

- V. O157:H7 and STm 14028s modulation of metabolic processes in leaves exhibited specificities and commonalities that are dependent upon plant species and time after inoculation.
- VI. Stimulation of changes in gene expression at the whole genome level in STm 14028s and O157:H7 is substantially larger in the first 4 h as compared to the subsequent 20 h after inoculation. This suggests a rapid reaction of the bacteria to the leaf apoplast environment and that most of these initial adjustments are maintained for at least the following 20 h.
- VII. Bacterial transcriptomic responses are substantially more extensive in *Arabidopsis* than in lettuce and modulation of gene expression is larger in STm 14028s than O157:H7. These results agree with the larger counter response induced in *Arabidopsis* than in lettuce. Moreover, variation in bacterial DEGs might have key roles in the differential ability of STm 14028s and O157:H7 to persist in the leaf apoplast between the two plant species.
- VIII. This study generated extensive functional genomics resources that can be further explored to test relevant hypothesis in the future.

Data availability

Raw sequencing data are available at the National Center for Biotechnology Information Short Read Archive, under the BioProject accession code PRJNA634120. Lists of DEGs and enriched GO terms of the treatments are listed in Dataset S01 and Dataset S02, respectively. Supplemental material available at figshare: <https://doi.org/10.25387/g3.16578644>.

Acknowledgments

We thank Cleverson Mantioli, James Kremer, and Sebastian Reyes-Chin-Wo for their technical support and Dr. R. Micheltore for providing the lettuce seeds and guidance on the growth of healthy lettuce plants.

M.M. and S.Y.H. conceived the research. C.J. performed the experiments. A.C.V. assisted with experimental design and troubleshooting. M.T. and N.A.J. conducted bioinformatics analysis. C.J. and M.M. designed the research, analyzed the data, and wrote the manuscript. All authors read and approved the manuscript.

Funding

This research was supported by grants from the U.S. Department of Agriculture—National Institute of Food and Agriculture (NIFA; 2015-67017-23360 to M.M. and S.Y.H., and 2017-67017-26180 to M.M.) and NIFA Hatch grant (CA-D-PLS-2327-H) to M.M. C.J. was supported by a BECAS-Chile [National Commission for Scientific and Technological Research(CONICYT)] fellowship and Horticulture and Agronomy Graduate Group fellowship from the University of California, Davis.

Conflicts of interest

The authors declare that they have no known competing financial interests or personal relationships that could have appeared to influence the work reported in this paper.

Literature cited

- AbuOun M, Suthers PF, Jones GI, Carter BR, Saunders MP, et al. 2009. Genome scale reconstruction of a salmonella metabolic model. comparison of similarity and differences with a commensal *Escherichia coli* strain. *J Biol Chem.* 284:29480–29488. doi: 10.1074/jbc.M109.005868.
- Aramaki T, Blanc-Mathieu R, Endo H, Ohkubo K, Kanehisa M, et al. 2020. KofamKOALA: KEGG ortholog assignment based on profile HMM and adaptive score threshold. *Bioinformatics.* 36: 2251–2252. pii:btz859. doi:10.1093/bioinformatics/btz859.
- Aranda PS, LaJoie DM, Jorcyk CL. 2012. Bleach gel: a simple agarose gel for analyzing RNA quality. *Electrophoresis.* 33:366–369. doi: 10.1002/elps.201100335.
- Ayala-Castro C, Saini A, Outten FW. 2008. Fe-S cluster assembly pathways in bacteria. *Microbiol Mol Biol Rev.* 72:110–125. doi: 10.1128/MMBR.00034-07.
- Barak JD, Jahn CE, Gibson DL, Charkowski AO. 2007. The role of cellulose and O-antigen capsule in the colonization of plants by *Salmonella enterica*. *Mol Plant Microbe Interact.* 20:1083–1091. doi: 10.1094/MPMI-20-9-1083.
- Benjamini Y, Hochberg Y. 1995. Controlling the false discovery rate: a practical and powerful approach to multiple testing. *J R Statist Soc.* 57:289–300. doi.org/10.1111/j.2517-6161.1995.tb02031.x.
- Bennett SD, Sodha SV, Ayers TL, Lynch MF, Gould LH, et al. 2018. Produce-associated foodborne disease outbreaks, USA, 1998–2013. *Epidemiol Infect.* 146:1397–1406. doi:10.1017/S0950268818001620.
- Bhagwat SP, Rice MR, Matthews RG, Blumenthal RM. 1997. Use of an inducible regulatory protein to identify members of a regulon: application to the regulon controlled by the leucine responsive regulatory protein (Lrp) in *Escherichia coli*. *J Bacteriol.* 179: 6254–6263. doi:10.1128/jb.179.20.6254-6263.1997.
- Brandl MT, Cox CE, Teplitski M. 2013. *Salmonella* interactions with plants and their associated microbiota. *Phytopathology.* 103: 316–325. doi:10.1094/PHYTO-11-12-0295-RVW.
- Brankatschk K, Kamber T, Pothier JF, Duffy B, Smits THM. 2014. Transcriptional profile of *Salmonella enterica* subsp. *enterica* serovar Weltevreden during alfalfa sprout colonization. *Microb Biotechnol.* 7:528–544. doi:10.1111/1751-7915.12104.
- Brichta-Harhay DM, Arthur TM, Bosilevac JM, Guerini MN, Kalchayanand N, et al. 2007. Enumeration of *Salmonella* and *Escherichia coli* O157:H7 in ground beef, cattle carcass, hide and faecal samples using direct plating methods. *J Appl Microbiol.* 103:1657–1668. doi:10.1111/j.1365-2672.2007.03405.x.
- Callejón RM, Rodríguez-Naranjo MI, Ubeda C, Hornedo-Ortega R, Garcia-Parrilla MC, et al. 2015. Reported foodborne outbreaks due to fresh produce in the United States and European Union: trends and causes. *Foodborne Pathog Dis.* 12:32–38. doi:10.1089/fpd.2014.1821.
- Chalupowicz L, Nissan G, Brandl MT, McClelland M, Sessa G, et al. 2018. Assessing the ability of *Salmonella enterica* to translocate type III effectors into plant cells. *Mol Plant Microbe Interact.* 31: 233–239. doi:10.1094/MPMI-07-17-0166-R.
- Chen L, Chu C, Lu J, Kong X, Huang T, et al. 2015. Gene ontology and KEGG pathway enrichment analysis of a drug target-based classification system. *PLoS One.* 10:e0126492. doi:10.1371/journal.pone.0126492.
- Cheng CY, Krishnakumar V, Chan AP, Thibaud-Nissen F, Schobel S, et al. 2017. Araport11: a complete reannotation of the *Arabidopsis thaliana* reference genome. *Plant J.* 89:789–804. doi:10.1111/tpj.13415.

- Cole J, Richardson D. 2008. Respiration of nitrate and nitrite. *EcoSal Plus*. 3:doi:10.1128/ecosal.3.2.5.
- Crozier L, Hedley PE, Morris J, Wagstaff C, Andrews SC, et al. 2016. Whole-transcriptome analysis of Verocytotoxigenic *Escherichia coli* O157:H7 (Sakai) suggests plant-species-specific metabolic responses on exposure to spinach and lettuce extracts. *Front Microbiol*. 7:1088. doi:10.3389/fmicb.2016.01088.
- De Cremer K, Mathys J, Vos C, Froenicke L, Michelmor RW, et al. 2013. Lettuce transcriptome during *Botrytis cinerea* infection. *Plant Cell Environ*. 36:1992–2007. doi:10.1111/pce.12106.
- Ditty JL, Grimm AC, Harwood CS. 1998. Identification of a chemotaxis gene region from *Pseudomonas putida*. *FEMS Microbiol Lett*. 159:267–273. doi:10.1111/j.1574-6968.1998.tb12871.x.
- Dixon RA, Achnine L, Kota P, Liu C-J, Reddy MSS, et al. 2002. The phenylpropanoid pathway and plant defense – a genomic perspective. *Mol Plant Pathol*. 3:371–390. doi:10.1046/j.1364-3703.2002.00131.x.
- Eichhorn E, van Der Ploeg JR, Leisinger T. 2000. Deletion analysis of the *Escherichia coli* taurine and alkanesulfonate transport systems. *J Bacteriol*. 182:2687–2795. doi:10.1128/jb.182.10.2687-2695.2000.
- Ferelli AMC, Bolten S, Szczesny B, Micallef SA. 2020. *Salmonella enterica* elicits and is restricted by nitric oxide and reactive oxygen species on tomato. *Front Microbiol*. 11:391. <https://www.frontiersin.org/article/10.3389/fmicb.2020.00391>.
- Figueira R, Holden DW. 2012. Functions of the *Salmonella* pathogenicity island 2 (SPI-2) type III secretion system effectors. *Microbiology (Reading)*. 158:1147–1161. doi:10.1099/mic.0.058115-0.
- Fink RC, Black EP, Hou Z, Sugawara M, Sadowsky MJ, et al. 2012. Transcriptional responses of *Escherichia coli* K-12 and O157:H7 associated with lettuce leaves. *Appl Environ Microbiol*. 78:1752–1764. doi:10.1128/AEM.07454-11.
- Flores-Kim J, Darwin AJ. 2016. The phage shock protein response. *Annu Rev Microbiol*. 70:83–101. doi:10.1146/annurev-micro-102215-095359.
- Garcia AV, Charrier A, Schikora A, Bigeard J, Pateyron S, et al. 2014. *Salmonella enterica* flagellin is recognized via FLS2 and activates PAMP-Triggered Immunity in *Arabidopsis thaliana*. *Mol Plant*. 7:657–674. doi:10.1093/mp/sst145.
- Gardner SG, Johns KD, Tanner R, McCleary WR. 2014. The PhoU protein from *Escherichia coli* interacts with PhoR, PstB, and metals to form a phosphate-signaling complex at the membrane. *J Bacteriol*. 196:1741–1752. doi:10.1128/JB.00029-14.
- Gaytán MO, Martínez-Santos VI, Soto E, González-Pedrajo B. 2016. Type three secretion system in attaching and effacing pathogens. *Front Cell Infect Microbiol*. 6:129. doi:10.3389/fcimb.2016.00129.
- Gopinath S, Carden S, Monack D. 2012. Shedding light on *Salmonella* carriers. *Trends Microbiol*. 20:320–327. doi:10.1016/j.tim.2012.04.004.
- Götz S, García-Gómez JM, Terol J, Williams TD, Nagaraj SH, et al. 2008. High-throughput functional annotation and data mining with the Blast2GO suite. *Nucleic Acids Res*. 36:3420–3435. doi:10.1093/nar/gkn176.
- Gupta M, Sharma G, Saxena D, Budhwar R, Vasudevan M, et al. 2020. Dual RNA-Seq analysis of *Medicago truncatula* and the pea powdery mildew *Erysiphe pisi* uncovers distinct host transcriptional signatures during incompatible and compatible interactions and pathogen effector candidates. *Genomics*. 112:2130–2145. doi:10.1016/j.ygeno.2019.12.007.
- Grandoni JA, Zahler SA, Calvo JM. 1992. Transcriptional regulation of the *ilv-leu* operon of *Bacillus subtilis*. *J Bacteriol*. 174:3212–3219. doi:10.1128/jb.174.10.3212-3219.1992.
- Haas BJ, Chin M, Nusbaum C, Birren BW, Livny J. 2012. How deep is deep enough for RNA-Seq profiling of bacterial transcriptomes? *BMC Genomics*. 13:734. doi:10.1186/1471-2164-13-734.
- Heberle H, Meirelles GV, da Silva FR, Telles GP, Minghim R. 2015. InteractiVenn: a web-based tool for the analysis of sets through Venn diagrams. *BMC Bioinformatics*. 16:169.
- Hernández-Reyes C, Schikora A. 2013. *Salmonella*, a cross-kingdom pathogen infecting humans and plants. *FEMS Microbiol Lett*. 343:1–7. doi:10.1111/1574-6968.12127.
- Hirt H. 2020. Healthy soils for healthy plants for healthy humans: how beneficial microbes in the soil, food and gut are interconnected and how agriculture can contribute to human health. *EMBO Rep*. 21:e51069. doi:10.15252/embr.202051069.
- Holden N, Pritchard L, Toth I. 2009. Colonization outwith the colon: plants as an alternative environmental reservoir for human pathogenic enterobacteria. *FEMS Microbiol Rev*. 33:689–703. doi:10.1111/j.1574-6976.2008.00153.x.
- Horswill AR, Escalante-Semerena JC. 2001. In vitro conversion of propionate to pyruvate by *Salmonella enterica* enzymes: 2-methylcitrate dehydratase (PrpD) and aconitase enzymes catalyze the conversion of 2-methylcitrate to 2-methylisocitrate. *Biochem*. 40:4703–4713. doi:10.1021/bi015503b.
- Huot B, Yao J, Montgomery BL, He SY. 2014. Growth–defense trade-offs in plants: a balancing act to optimize fitness. *Mol Plant*. 7:1267–1287. doi:10.1093/mp/ssu049.
- Jacob C, Melotto M. 2019. Human pathogen colonization of lettuce dependent upon plant genotype and defense response activation. *Front Plant Sci*. 10:1769. doi:10.3389/fpls.2019.01769.
- Jacob C, Panchal S, Melotto M. 2017. Surface inoculation and quantification of *Pseudomonas syringae* population in the *Arabidopsis* leaf apoplast. *Bioprotocol*. 7:e2167. doi.org/10.21769/BioProtoc.2167.
- Javelle A, Merrick M. 2005. Complex formation between AmtB and GlnK: an ancestral role in prokaryotic nitrogen control. *Biochem Soc Trans*. 33:170–172. doi:10.1042/BST0330170.
- Jayaraman D, Valdés-López O, Kaspar CW, Ané JM. 2014. Response of *Medicago truncatula* seedlings to colonization by *Salmonella enterica* and *Escherichia coli* O157:H7. *PLoS One*. 9:e87970. doi:10.1371/journal.pone.0087970.
- Jechalke S, Schierstaedt J, Becker M, Flemer B, Grosch R, et al. 2019. *Salmonella* establishment in agricultural soil and colonization of crop plants depend on soil type and plant species. *Front Microbiol*. 10:967. doi:10.3389/fmicb.2019.00967.
- Jo SH, Park JM. 2019. The dark side of organic vegetables: interactions of human enteropathogenic bacteria with plants. *Plant Biotechnol Rep*. 13:105–110. doi:10.1007/s11816-019-00536-1.
- Jochimsen B, Lolle S, McSorley FR, Nabi M, Stougaard J, et al. 2011. Five phosphonate operon gene products as components of a multi-subunit complex of the carbon-phosphorus lyase pathway. *Proc Natl Acad Sci U S A*. 108:11393–11398. doi:10.1073/pnas.1104922108.
- Kanehisa M, Sato Y. 2020. KEGG Mapper for inferring cellular functions from protein sequences. *Protein Sci*. 29:28–35. doi:10.1002/pro.3711.
- Katagiri F, Thilmony R, He SY. 2002. The *Arabidopsis thaliana*-*Pseudomonas syringae* interaction. *Arabidopsis Book*. 1:e0039. doi:10.1199/tab.0039.
- Kaval KG, Garsin DA. 2018. Ethanolamine utilization in bacteria. *mBio*. 9:e00066–18. doi:10.1128/mBio.00066-18.
- Kyle JL, Parker GT, Goudeau D, Brandl MT. 2010. Transcriptome analysis of *Escherichia coli* O157:H7 exposed to lysates of lettuce leaves. *Appl Environ Microbiol*. 76:1375–1387. doi:10.1128/AEM.02461-09.

- Landstorfer R, Simon S, Schober S, Keim D, Scherer D, et al. 2014. Comparison of strand-specific transcriptomes of enterohemorrhagic *Escherichia coli* O157:H7 EDL933 (EHEC) under eleven different environmental conditions including radish sprouts and cattle feces. *BMC Genomics*. 15:353. doi:10.1186/1471-2164-15-353.
- Law CW, Alhamdoosh M, Su S, Dong X, Tian L, et al. 2018. RNA-seq analysis is easy as 1-2-3 with limma, Glimma and edgeR. *F1000Res*. 5:1408. doi:10.12688/f1000research.9005.3.
- Lex A, Gehlenborg N, Strobel H, Vuillemot R, Pfister H. 2014. UpSet: visualization of intersecting sets. *IEEE Trans Vis Comput Graph*. 20:1983–1992. doi:10.1109/TVCG.2014.2346248.
- Liu R, Ochman H. 2007. Origins of flagellar gene operons and secondary flagellar systems. *J Bacteriol*. 189:7098–7104. doi:10.1128/JB.00643-07.
- Lucier G, Parr B. 2020. Vegetable and Pulses Outlook, VGS-364, U.S. Department of Agriculture, Economic Research Service. <https://www.ers.usda.gov/webdocs/outlooks/98295/vgs-364.pdf?v=5113>(Accessed: January 4, 2021).
- Macarasin D, Patel J, Bauchan G, Giron JA, Ravishankar S. 2013. Effect of spinach cultivar and bacterial adherence factors on survival of *Escherichia coli* O157:H7 on spinach leaves. *J Food Prot*. 76:1829–1837. doi:10.4315/0362-028X.JFP-12-556.
- Marsh JW, Hayward RJ, Shetty AC, Mahurkar A, Humphrys MS, et al. 2018. Bioinformatic analysis of bacteria and host cell dual RNA-sequencing experiments. *Brief Bioinform*. 19:1115–1115. doi:10.1093/bib/bbx043.
- Marshall KE, Hexemer A, Seelman SL, Fatica MK, Blessington T, et al. 2020. Lessons learned from a decade of investigations of Shiga toxin-producing *Escherichia coli* outbreaks linked to leafy greens, United States and Canada. *Emerg Infect Dis*. 26:2319–2328. doi:10.3201/eid2610.191418.
- Melotto M, Panchal S, Roy D. 2014. Plant innate immunity against human bacterial pathogens. *Front Microbiol*. 5:411–12. doi:10.3389/fmicb.2014.00411.
- Meyer FE, Shuey LS, Naidoo S, Mamni T, Berger DK, et al. 2016. Dual RNA sequencing of *Eucalyptus nitens* during *Phytophthora cinnamomi* challenge reveals pathogen and host factors influencing compatibility. *Front Plant Sci*. 7:191. doi:10.3389/fpls.2016.00191.
- Mi H, Ebert D, Muruganujan A, Mills C, Albu L-P, et al. 2021. PANTHER version 16: a revised family classification, tree-based classification tool, enhancer regions and extensive API. *Nucleic Acids Res*. 49:D394–D403. doi:10.1093/nar/gkaa1106.
- Montano J, Rossidivito G, Torreano J, Porwollik S, Sela (Saldinger) S, et al. 2020. *Salmonella enterica* serovar Typhimurium 14028s genomic regions required for colonization of lettuce leaves. *Front Microbiol*. 11:6. doi:10.3389/fmicb.2020.00006.
- Monterrubio R, Baldoma L, Obradors N, Aguilar J, Badia J. 2000. a common regulator for the operons encoding the enzymes involved in d-galactarate, d-glucarate, and d-glycerate utilization in *Escherichia coli*. *J Bacteriol*. 182:2672–2674. doi:10.1128/jb.182.9.2672-2674.2000.
- Nobori T, Velásquez AC, Wu J, Kvitko BH, Kremer JM, et al. 2018. Transcriptome landscape of a bacterial pathogen under plant immunity. *Proc Natl Acad Sci U S A*. 115:E3055–E3064. doi.org/10.1073/pnas.1800529115.
- Parales RE, Ingraham JL. 2010. The surprising Rut pathway: an unexpected way to derive nitrogen from pyrimidines. *J Bacteriol*. 192:4086–4088. doi:10.1128/JB.00573-10.
- Pereira CS, Thompson JA, Xavier KB. 2013. AI-2-mediated signalling in bacteria. *FEMS Microbiol Rev*. 37:156–181. doi:10.1111/j.1574-6976.2012.00345.x.
- Phoebe C, Catherine L, Lee A. 2001. The *Salmonella* pathogenicity island-1 type III secretion system. *Microb Infect*. 3:1281–1291. doi:10.1016/S1286-4579(01)01488-5.
- Porwollik S, Santiviago SA, Cheng P, Long F, Desai P, et al. 2014. Defined single-gene and multi-gene deletion mutant collections in *Salmonella enterica* sv Typhimurium. *PLoS One*. 9:e99820. doi:10.1371/journal.pone.0099820.
- Preiss L, Hicks DB, Suzuki S, Meier T, Krulwich TA. 2015. Alkaliphilic bacteria with impact on industrial applications, concepts of early life forms, and bioenergetics of ATP synthesis. *Front Bioeng Biotechnol*. 3:75. doi:10.3389/fbioe.2015.00075.
- Reyes-Chin-Wo S, Wang Z, Yang X, Kozik A, Arikat S, et al. 2017. Genome assembly with in vitro proximity ligation data and whole-genome triplication in lettuce. *Nat Commun*. 8:14953. doi:10.1038/ncomms14953.
- Ritchie ND, Evans TJ. 2019. Dual RNA-seq in *Streptococcus pneumoniae* infection reveals compartmentalized neutrophil responses in lung and pleural space. *mSystems*. 4:e00216–19. doi:10.1128/mSystems.00216-19.
- Rivera-Chávez F, Bäumler AJ. 2015. The pyromaniac inside you: *Salmonella* metabolism in the host gut. *Annu Rev Microbiol*. 69:31–48. doi:10.1146/annurev-micro-091014-104108.
- Römling U, Galperin MY. 2015. Bacterial cellulose biosynthesis: diversity of operons, subunits, products and functions. *Trends Microbiol*. 23:545–557. doi:10.1016/j.tim.2015.05.005.
- Roy D, Panchal S, Rosa BA, Melotto M. 2013. *Escherichia coli* O157:H7 induces stronger plant immunity than *Salmonella enterica* Typhimurium SL1344. *Phytopathology*. 103:326–332. doi:10.1094/PHYTO-09-12-0230-FI.
- Saliba AE, Santos SC, Vogel J. 2017. New RNA-seq approaches for the study of bacterial pathogens. *Curr Opin Microbiol*. 35:78–87. doi:10.1016/j.mib.2017.01.001.
- Saldaña Z, Sánchez E, Xicohtencatl-Cortes J, Puente JL, Girón JA. 2011. Surface structures involved in plant stomata and leaf colonization by Shiga-toxigenic *Escherichia coli* O157:H7. *Front Microbiol*. 2:119. doi:10.3389/fmicb.2011.00119.
- Sapers GM, Doyle MP. 2014. Chapter 1—Scope of the produce contamination problem. In: KR Matthews, GM Sapers, CP Gerba, editors. *The Produce Contamination Problem: Causes and Solutions*, 2nd ed. Amsterdam, Netherlands: Elsevier. p. 3–20, 467.
- Schikora A, Carreri A, Charpentier E, Hirt H. 2008. The dark side of the salad: *Salmonella typhimurium* overcomes the innate immune response of *Arabidopsis thaliana* and shows an endopathogenic lifestyle. *PLoS One*. 3:e2279. doi:10.1371/journal.pone.0002279.
- Schikora A, Virlogeux-Payant I, Bueso E, Garcia AV, Nilau T, et al. 2011. Conservation of *Salmonella* infection mechanisms in plants and animals. *PLoS One*. 6:e24112. doi:10.1371/journal.pone.0024112.
- Shirron N, Yaron S. 2011. Active suppression of early immune response in tobacco by the human pathogen *Salmonella* Typhimurium. *PLoS One*. 6:e18855. doi:10.1371/journal.pone.0018855.
- Smith OM, Snyder WE, Owen JP. 2020. Are we overestimating risk of enteric pathogen spillover from wild birds to humans? *Biol Rev Camb Philos Soc*. 95:652–679. doi:10.1111/brv.12581.
- Sperandio V, Torres AG, Girón JA, Kaper JB. 2001. Quorum sensing is a global regulatory mechanism in enterohemorrhagic *Escherichia coli* O157:H7. *J Bacteriol*. 183:5187–5197. doi:10.1128/JB.183.17.5187-5197.2001.
- Srikumar S, Fuchs TM. 2011. Ethanolamine utilization contributes to proliferation of *Salmonella enterica* serovar Typhimurium in food and in nematodes. *Appl Environ Microbiol*. 77:281–290. doi:10.1128/AEM.01403-10.

- Srivastava D, Shamim M, Kumar M, Mishra A, Maurya R, et al. 2019. Role of circadian rhythm in plant system: an update from development to stress response. *Environ Exp Bot.* 162:256–271. doi:10.1016/j.envexpbot.2019.02.025.
- Stewart V, Lu Y, Darwin AJ. 2002. Periplasmic nitrate reductase (NapABC enzyme) supports anaerobic respiration by *Escherichia coli* K-12. *J Bacteriol.* 184:1314–1323. doi:10.1128/JB.184.5.1314-1323.2002.
- Taylor L, Nunes-Nesi A, Parsley K, Leiss A, Leach G, et al. 2010. Cytosolic pyruvate, orthophosphate dikinase functions in nitrogen remobilization during leaf senescence and limits individual seed growth and nitrogen content. *Plant J.* 62:641–652. doi:10.1111/j.1365-313X.2010.04179.x.
- Thilmony R, Underwood W, He SY. 2006. Genome-wide transcriptional analysis of the *Arabidopsis thaliana* interaction with the plant pathogen *Pseudomonas syringae* pv. tomato DC3000 and the human pathogen *Escherichia coli* O157:H7. *Plant J.* 46:34–53. doi:10.1111/j.1365-313X.2006.02725.x.
- Thimm T, Bläsing O, Gibon Y, Nagel A, Meyer S, et al. 2004. MAPMAN: a user-driven tool to display genomics data sets onto diagrams of metabolic pathways and other biological processes. *Plant J.* 37:914–939. doi:10.1111/j.1365-313X.2004.02016.x.
- Turner K, Moua CN, Hajmeer M, Barnes A, Needham M. 2019. Overview of leafy greens-related food safety incidents with a California link: 1996 to 2016. *J Food Prot.* 82:405–414. doi:10.4315/0362-028X.JFP-18-316.
- Ueno-Nishio S, Backman KC, Magasanik B. 1983. Regulation at the *glnL*-operator-promoter of the complex *glnALG* operon of *Escherichia coli*. *J Bacteriol.* 153:1247–1251. doi:10.1128/JB.153.3.1247-1251.
- Uden G, Steinmetz PA, Degreif-, Dünwald P. 2014. The aerobic and anaerobic respiratory chain of *Escherichia coli* and *Salmonella enterica*: enzymes and energetics. *EcoSal Plus.* 6: doi:10.1128/ecosal-plus.ESP-0005-2013.
- Valenzuela-Miranda D, Gallardo-Escárate C. 2018. Dual RNA-Seq uncovers metabolic amino acids dependency of the intracellular bacterium *Piscirickettsia salmonis* infecting Atlantic salmon. *Front Microbiol.* 9:2877. doi:10.3389/fmicb.2018.02877.
- Van der Linden I, Cottyn B, Uyttendaele M, Vlaemynck G, Heyndrickx M, et al. 2016. Microarray-based screening of differentially expressed genes of *E. coli* O157:H7 Sakai during preharvest survival on butterhead lettuce. *Agriculture.* 6:6. doi:10.3390/agriculture6010006.
- van Heeswijk WC, Westerhoff HV, Booger FC. 2013. Nitrogen assimilation in *Escherichia coli*: putting molecular data into a systems perspective. *Microbiol Mol Biol Rev.* 77:628–695. doi:10.1128/MMBR.00025-13.
- Wang D, Dong X. 2011. A highway for war and peace: the secretory pathway in plant-microbe interactions. *Mol Plant.* 4:581–587. doi:10.1093/mp/ssr053.
- Wang H, Gunsalus RP. 2000. The *nrfA* and *nirB* nitrite reductase operons in *Escherichia coli* are expressed differently in response to nitrate than to nitrite. *J Bacteriol.* 182:5813–5822. doi:10.1128/JB.182.20.5813-5822.2000.
- Wechsler JA, Adelberg EA. 1969. Antipolarity in the *ilv* operon of *Escherichia coli* K-12. *J Bacteriol.* 98:1179–1194.
- Westermann AJ, Barquist L, Vogel J. 2017. Resolving host-pathogen interactions by dual RNA-seq. *PLoS Pathog.* 13:e1006033. doi:10.1371/journal.ppat.1006033.
- World Health Organization [WHO]. 2015. WHO Estimates of the Global Burden of Foodborne Diseases: Foodborne Disease Burden Epidemiology Reference Group 2007–2015. Geneva: World Health Organization.
- Wu H, Chen S, Ji M, Chen Q, Shi J, et al. 2019. Activation of colanic acid biosynthesis linked to heterologous expression of the polyhydroxybutyrate pathway in *Escherichia coli*. *Int J Biol Macromol.* 128:752–760. doi:10.1016/j.ijbiomac.2019.02.004.
- Yanofsky C, Horn V. 1994. Role of regulatory features of the *trp* operon of *Escherichia coli* in mediating a response to a nutritional shift. *J Bacteriol.* 176:6245–6254. doi:10.1128/jb.176.20.6245-6254.
- Yaron S, Römling U. 2014. Biofilm formation by enteric pathogens and its role in plant colonization and persistence. *Microb Biotechnol.* 7:496–516. doi:10.1111/1751-7915.12186.
- Zarkani AA, López-Pagán N, Grimm M, Sánchez-Romero MA, Ruiz-Albert J, et al. 2020. *Salmonella* heterogeneously expresses flagellin during colonization of plants. *Microorganisms.* 8:815. doi:10.3390/microorganisms8060815.
- Zhou M, Guo Z, Duan Q, Hardwidge PR, Zhu G. 2014. *Escherichia coli* type III secretion system 2: a new kind of T3SS? *Vet Res.* 45:32. <http://www.veterinaryresearch.org/content/45/1/32>.

Communicating editor: B. Andrews